Reconstruction of geomagnetic activity and near-Earth interplanetary conditions over the past 167 yr – Part 1: A new geomagnetic data composite

Article

Published Version

Lockwood, M. ORCID: https://orcid.org/0000-0002-7397-2172, Barnard, L., Nevanlinna, H., Owens, M.J. ORCID: https://orcid.org/0000-0003-2061-2453, Harrison, R.G. ORCID: https://orcid.org/0000-0003-0693-347X, Rouillard, A. P. and Davis, C. J. ORCID: https://orcid.org/0000-0001-6411-5649

www.reading.ac.uk/centaur

CentAUR

Central Archive at the University of Reading

Reading's research outputs online

Annales
Geophysicae

Reconstruction of geomagnetic activity and near-Earth interplanetary conditions over the past 167 yr – Part 1: A new geomagnetic data composite

M. Lockwood[1], L. Barnard[1], H. Nevanlinna[2], M. J. Owens[1], R. G. Harrison[1], A. P. Rouillard[3], and C. J. Davis[1]

[1]Meteorology Department, University of Reading, Reading, Berkshire, UK
[2]Finnish Meteorological Institute, P.O. Box 503, 00101 Helsinki, Finland
[3]Institut de Recherché en Astrophysique et Planétologie, 9 Ave. du Colonel Roche,
BP 44 346, 31028 Toulouse Cedex 4, France

Correspondence to: M. Lockwood (m.lockwood@reading.ac.uk)

Abstract. We present a new composite of geomagnetic activity which is designed to be as homogeneous in its construction as possible. This is done by only combining data that, by virtue of the locations of the source observatories used, have similar responses to solar wind and IMF (interplanetary magnetic field) variations. This will enable us (in Part 2, Lockwood et al., 2013a) to use the new index to reconstruct the interplanetary magnetic field, *B*, back to 1846 with a full analysis of errors. Allowance is made for the effects of secular change in the geomagnetic field. The composite uses interdiurnal variation data from Helsinki for 1845–1890 (inclusive) and 1893–1896 and from Eskdalemuir from 1911 to the present. The gaps are filled using data from the Potsdam (1891–1892 and 1897–1907) and the nearby Seddin observatories (1908–1910) and intercalibration achieved using the Potsdam–Seddin sequence. The new index is termed IDV(1d) because it employs many of the principles of the IDV index derived by Svalgaard and Cliver (2010), inspired by the *u* index of Bartels (1932); however, we revert to using one-day (1d) means, as employed by Bartels, because the use of near-midnight values in IDV introduces contamination by the substorm current wedge auroral electrojet, giving noise and a dependence on solar wind speed that varies with latitude. The composite is compared with independent, early data from European-sector stations, Greenwich, St Petersburg, Parc St Maur, and Ekaterinburg, as well as the composite *u* index, compiled from 2–6 stations by Bartels, and the IDV index of Svalgaard and Cliver. Agreement is found to be extremely good in all cases, except two. Firstly, the Green-

wich data are shown to have gradually degraded in quality until new instrumentation was installed in 1915. Secondly, we infer that the Bartels *u* index is increasingly unreliable before about 1886 and overestimates the solar cycle amplitude between 1872 and 1883 and this is amplified in the proxy data used before 1872. This is therefore also true of the IDV index which makes direct use of the *u* index values.

Keywords. Interplanetary physics (Instruments and techniques)

1 Introduction

This paper generates a geomagnetic index that is homogeneous in its construction, such that it is suitable for use when reconstructing past variations in solar wind parameters. All such reconstructions rely on correlations between near-Earth interplanetary parameters and the geomagnetic index during the space age and, implicitly or explicitly, make the assumption that the response of the index was the same at all times before the space age (see review by Lockwood, 2013). It is therefore important to construct the index in such a way that its response to solar wind variations remains, as far as is practically possible, constant over time. We here refer to such an index as "homogeneously constructed". The response of any one geomagnetic observatory to near-Earth interplanetary variations depends on a number of factors including (1) the instrumentation used, (2) the calibrations procedures used, (3) local site characteristics, (4) the Universal Time

(UT), (5) the geographic latitude, (6) the Solar Local Time (SLT), (7) the Magnetic Local Time (MLT) and (8) the geomagnetic latitude. Important UT dependencies arise because of the offsets between the geomagnetic and rotation axes of the Earth which influences factors such as the magnetic shear across the dayside magnetopause for a given interplanetary magnetic field (Russell and McPherron, 1973; Russell, 1989; Nowada et al., 2009) and the degree of bending of the mid-tail of the magnetosphere (Kivelson and Hughes, 1990). The geographic latitude and SLT are factors because of the spatial distribution of EUV (extreme ultraviolet)-generated ionospheric conductivities (e.g. Moen and Brekke, 1993; Wallis and Budzinski, 1981) and of thermally driven winds in the thermosphere (e.g. Brum et al., 2012; Yamazaki et al., 2011) and the MLT and geomagnetic latitude determine the location of the station relative to key influential parts of the near-Earth current systems such as the magnetospheric ring current and the substorm current wedge auroral electrojet (see review by Lockwood, 2013). To ensure that the combination of factors 4–8 stay as constant as possible, the spatial distribution of stations employed should change as little as possible. In the absence of continuously operating observatories over the full period, data from stations with similar responses to interplanetary changes should be splined together into a composite and factors 1–3 require that robust intercalibrations are used. However, even where we have continuous data from one geographic location, the secular change in the geomagnetic field means that there are long-term drifts in its magnetic coordinates, changing the response to solar wind forcing and changing quiet time thermospheric winds and geomagnetic disturbances (Cnossen and Richmond, 2013). Long-term change in Earth's magnetic moment influences the solar wind–magnetosphere coupling efficiency (Stamper et al., 1999). Allowance for the effect of the change in stations' geomagnetic coordinates requires use of a historic geomagnetic field model and the development of an algorithm to remove the effects of the secular drifts. To understand these issues in more detail we here look at existing long-term geomagnetic indices.

1.1 The *aa* index

For many years, the only available long-term record of geomagnetic activity was the *aa* index, compiled for 1868–1968 by Mayaud (1971, 1972, 1980) and subsequently continued to the present day. This is a "range" index, meaning that it is based on "*k* indices" which, in turn, are derived from the range of variation of the horizontal component of Earth's field (H) detected by ground-based magnetometers in 3 h intervals. To compile *aa*, Mayaud used two antipodal stations, one in southern England one in Australia; however, to obtain continuous sequences, data from three observatory sites were needed in both hemispheres. For the Northern Hemisphere the sites used were Greenwich (1868–1925), Abinger (1926–1956) and Hartland (1957–present), and for the Southern

Hemisphere they were Melbourne (1868–1918), Toolangi (1919–1979) and Canberra (1980–present). In most cases, the site changes were necessary because urbanisation around the original observatories greatly increased the noise level and/or changed their magnetic properties. In each case, available overlap data were used to intercalibrate the data sequences. The Northern and Southern Hemisphere data yield aa_N and aa_S, respectively, and *aa* is the arithmetic mean of the two. Mayaud intended *aa* to be used on annual timescales and showed that its annual means correlated exceptionally well with Ap which is a range index compiled from 11–13 stations in the Northern Hemisphere (plus Eyrewell and Canberra, or their equivalents, in the south) since 1936. An extension of *aa* back to 1846 was made by Nevanlinna and Kataja (1993) using the range *k* index data from the Helsinki Observatory.

The most interesting feature of *aa* is that it shows a significant upward drift throughout most of the 20th century (comparable to modern solar cycle amplitudes). It has been argued that this was caused by either secular change in the geomagnetic field site or instrument changes or station intercalibration errors. There are indeed a great many ways in which a magnetometer site's characteristics can change: these include changes in the local water table, the installation of nearby power lines, railways and tramways and constructions with considerable metallic content. However, none of these potential errors provides a viable explanation of most of the upward drift in *aa*. Much of the rise is seen after 1936 and is also found in the Ap index which uses stations at all longitudes (and so the secular change in the geomagnetic field has caused some to rise and some to fall in geomagnetic latitude). Using the IGRF model of the geomagnetic field, Clilverd et al. (1998) pointed out that the Northern Hemisphere *aa* stations have drifted about 4° equatorward in geomagnetic latitude since 1900 whereas the Southern Hemisphere stations have drifted about 2° poleward, yet aa_N and aa_S show very similar behaviour, both in their solar cycle variations and their long-term drift (Lockwood, 2003; Love, 2011). This is not to say that the Northern and Southern Hemisphere stations give identical data and are perfectly intercalibrated (e.g. Love, 2011). It is now generally agreed that there is a calibration error in the standard version of *aa* (as stored in many data centres) associated with the move of the Northern Hemisphere station from Abinger to Hartland in 1957 and that this accounts for 25 % of the rise in *aa* before the start of the space age, leaving 75 % due to changes in the Sun (see review by Lockwood, 2013). However, many of the other differences are apparent only on timescales below 1 yr (and Mayaud never intended *aa* to be used on anything shorter than annual timescales). The majority of the long-term drift in *aa* cannot be attributed to site changes, nor to the intercalibration of stations, nor to changes in the sensitivity of the stations in both hemispheres (Clilverd et al., 1998; Love, 2011). Stamper et al. (1999) analysed all the potential factors that could have induced the solar cycle variations and long-term

drift in *aa* since the start of the space age and concluded that the only viable explanation was variation in near-Earth interplanetary space caused by changes in the solar corona. The debate about the potential for long-term changes in *aa*, comparable in magnitude to the solar cycle amplitude, has been dramatically ended by the recent "exceptional" solar minimum (Lockwood, 2010). A decline in solar and geomagnetic activity since 1985 was noted by Lockwood (2003) and the low solar minimum between cycles 23 and 24 was a continuation of that decline, such that by 2013, the 22 yr mean in *aa* has fallen by almost a full solar cycle amplitude and most of the rise between 1900 and 1985, has already been matched by the fall since 1985 (Lockwood et al., 2012).

Note that Mayaud had data available to him that he did not employ in the *aa* index (including, for example, the data that was used to compile the multi-station *Ap* index after 1936). The reason he did not use these other data was because to do so would have rendered the *aa* index inhomogeneous in its construction. Instead, Mayaud used just one site in southern England and one site in southern Australia throughout the 1868–1968 interval he studied.

The *aa* index has been used by several authors to make deductions about long-term change in the solar wind (Feynman and Crooker, 1978, Lockwood et al., 1999; Lockwood et al., 2009). Such reconstructions are the subject of Part 2 (Lockwood et al., 2013a). However, range indices, such as *aa*, are not easily re-generated for historical data and cannot be derived from most of the data stored in observatory yearbooks. Even when paper records of historic magnetograms are available, factors such as shrinkage of the paper charts with time can make their scaling not straightforward. Hence there have been recent attempts to generate geomagnetic indices from hourly means of data or hourly samples ("spot values") which were often recorded in the observatory yearbooks. Three examples of this are the median index *m*, as implemented by Lockwood et al. (2006b) and used by Rouillard et al. (2007); the inter-hour variability (IHV) index proposed by Svalgaard and Cliver (2007) and Svalgaard et al. (2003); and the interdiurnal variation (IDV) index introduced by Svalgaard and Cliver (2005) (hereafter SC05), and developed by Svalgaard and Cliver (2010) (hereafter SC10). These indices, and IDV in particular, have opened up the application of many historic data and, as a result, the *aa* index is no longer the only centennial record of geomagnetic activity.

1.2 The IHV index

The IHV index was proposed by Svalgaard et al. (2004) and developed by Svalgaard et al. (2003) and Svalgaard and Cliver (2007). It provides an example of how the need for robust and accurate correlations of data from different stations can conflict with the requirement for homogeneous index construction. IHV for a given station is defined as the sum of the absolute values of the difference between hourly means for a specified geomagnetic component from

1 h to the next over the 7 h interval around local midnight. Lockwood (2013) showed that IHV, like *aa*, depends on BV^2 (where B is the near-Earth interplanetary magnetic field strength and V is the solar wind speed) because it is strongly influenced by the substorm current wedge. Hence it is valid to compare *aa* and IHV. The original form of IHV by Svalgaard et al. (2004) was homogeneous in its construction because it used just two stations in close proximity (Cheltenham and Fredericksburg) and hence the only inhomogeneity is the secular drift in the geomagnetic coordinates of these stations. However, the overlap of the operation of these two stations is just three quarters of 1 yr (1956) and the intercalibration between the two used by Svalgaard et al. (2004) was so poor that they attributed all of the long-term change in *aa* to a calibration error in *aa* of over 8 nT (around 1957, i.e. the same time as the larger calibration glitch in the original IDV) and so wrongly concluded that there was no change at all in solar and interplanetary magnetic fields. Using other stations, Mursula et al. (2004) found that the calibration of this original version of IHV was indeed poor and so Svalgaard et al. (2003) revised their estimates using more stations (lowering their estimate of the calibration error in *aa* to 5.2 nT and so acknowledging for the first time that at least some of the drift in *aa* was solar in origin). However, Mursula and Martini (2006) showed that about half of this difference was actually caused by an inhomogeneity in the IHV data series, namely that Svalgaard et al. (2003) had used spot values for the early years and hourly means in later years. This was corrected by Svalgaard and Cliver (2007), who revised their estimate of the calibration error in *aa* further downward to 3 nT (showing 75 % of the drift in *aa* is of solar origin). The use of spot values was an obvious inhomogeneity in the construction of IHV that caused a major and obvious error in reconstructing interplanetary conditions. However there is a more subtle second inhomogeneity introduced by the use of many stations to overcome the calibration problem and that is the spatial distribution of the stations employed changes with time and, as noted for IHV by Mursula and Martini (2006), the geomagnetic response of the index depends on the station's location. Hence using variable distributions of stations introduces changes in the index response to interplanetary variations. Thus the initial version of IHV was homogeneous in its construction, but it contained a major calibration error. Later versions of IHV use more stations to reduce such calibration errors but, because the distribution and number of station changes with time, the index is no longer homogeneous in construction. This means that the response to changes in near-Earth interplanetary space will have changed and so we cannot have confidence that correlations derived in the space age are equally valid at earlier times. In this way, inhomogeneities in the construction of the geomagnetic index introduce unknown and undetected errors into the reconstructions of interplanetary and solar parameters.

1.3 The IDV index

The inspiration for IDV is the *u* index of Bartels (1932) which was defined as the weighted means of data, from a variety of stations, on the absolute value of the difference between the mean values of *H* or *Z* (whichever yields the larger value) for a day and for the preceding day. The main difference between *u* and IDV is that, in order to further suppress contamination by changes in the regular diurnal variation (most, but not all, of which is removed from *u* by taking daily means), IDV uses only the hourly means (or spot values) for the UT when the station in question was closest to local midnight. Bartels' work on the *u* index was criticised at the time for failing to register the recurrent geomagnetic storms and, as a result, he himself developed the range indices as an alternative (Bartels et al., 1939). However, as pointed out by SC05, this feature is a positive advantage of *u* as it means that it does not respond strongly, if at all, to solar wind speed variations, as will be discussed in Part 2. As a result, IDV offers a way of directly determining the interplanetary magnetic field which can be readily applied to a great deal of recorded historic data. One potential inhomogeneity in the data series is that most of the older observatory yearbooks contain spot values taken once every hour rather than the hourly means available in later years. SC10 have analysed the IDV data sequence and (unlike for IHV, as discussed in the previous section) can find no discontinuities associated with the change from spot to hourly mean data, but one should remain aware of the change.

SC05 find a $1/\cos^{0.7}(\Lambda)$ dependence of IDV from different stations, where Λ is the corrected geomagnetic latitude, and they use this to normalise the data (they follow Bartels and normalise to the Λ of the Niemegk station) before they are averaged together. The number of stations used in the IDV generated by SC05 was 34 for 1964–2003, but roughly half of these were discarded because of auroral contamination, and the number decreased going back in time such that there were just 5 in 1903 and only one (Potsdam) for 1890–1901. SC05 extended the sequence back to 1872 using Bartels' *u* index which correlates extremely well with IDV over the interval 1890–1930 ($r = 0.95$ for annual means). Bartels used a $1/\cos(\Lambda_D)$ dependence (rather than the $1/\cos^{0.7}(\Lambda)$ used in IDV, where Λ_D and Λ are, respectively, the dipole and corrected geomagnetic latitudes) and data from Seddin (1905–1928), Potsdam (1891–1904), Greenwich (1872–1890), Bombay (1872–1920), Batavia (1884–1899 and 1902–1926), Honolulu (1902–1930), Puerto Rico (1902–1916), Tucson (1917–1930), and Watheroo (1919–1930). It is interesting that Bartels notes the stability problems with the Greenwich data in deriving interdiurnal variation data and ascribes half weighting to it as a result. In addition, he notes some data gaps in the Bombay data and so also ascribes half weight to them at certain times. As a result *u* is, effectively, based on 1.5 stations for 1872–1891, rising to 6 by 1919 before falling to 3 again by 1930.

In an updated version of IDV, SC10 added data from more stations, such that the number exceeds 50 for most of the space age, is 23 for 1955 (prior to the growth in the global network associated with the International Geophysical Year, IGY), falling to just one in 1880. SC10 also extended this reconstruction back to 1835 which is just 3 yr after Gauss' establishment of the first magnetometer station in Göttingen. The data for 1835–1872 was compiled by Bartels and is called the *u* index but is not the same as *u* available after 1872. Bartels notes that before 1872, no proper data to generate an interdiurnal index was available to him and so other correlated measures of the diurnal variation are used as proxies. Bartels himself stresses that the *u* values before 1872 are "more for illustration than for actual use" and describes data for 1835–1847 as "least reliable", 1847–1872 as "better" and 1872–1930 as "satisfactory". Given that Bartels does not include his data before 1872 in his "satisfactory" grouping, it is not just a semantic point that he regarded the data before 1872 as "unsatisfactory". SC10 carried out some tests to justify employing the *u* proxy data for before 1872 in order to reconstruct geomagnetic activity back to 1835. We here make two points about those tests. Firstly they show that the proxy data can explain $r^2 = 0.72$ of the IDV variation over the interval 1883–2008 (i.e. including long-term drift and solar cycle oscillations) but there is 28 % of the IDV variation that is not explained by the proxy. The differences between SC10's IDV and the new IDV(1d) derived here before 1872 are always less than 32 % and typically half this value. Even this maximum is only slightly larger than the uncertainty introduced into IDV by the use of the proxy. In addition, the SC10 tests tell us nothing about the error in Bartels' early proxy data that caused him to class the *u* values derived from them as unsatisfactory, as discussed above. In conclusion the IDV index is not homogeneous in construction, because the number of stations is lower in the early years, because the geographical distribution of stations changes and particularly because it employs proxy data from before 1872.

SC05 and SC10 looked at the response of the composite (multi-station) IDV index to solar wind forcing and did not look at that for each of the individual stations. We here show that there is a systematic difference with latitude of the peak correlation with BV^n (where B is the interplanetary magnetic field and V is the solar wind speed), it being near $n = -0.2$ at the geomagnetic equator (close to the dependence of the ring current revealed by the negative part of Dst, see Lockwood, 2013), rising to n near $+0.4$ at $50°$ corrected geomagnetic latitude (introduced by the auroral electrojet, as discussed by Lockwood, 2013). In addition, we have defined other site-dependent dependencies of the response – for example on the size of the local field and on the station longitude (as would be expected because of the UT effect introduced by the dipole tilt effect of the Earth). This means that the net response of the IDV composite index changes with time because the number and distribution of stations changes with time. Thus the correlations with B and V (or

some combination thereof) derived in the space age have increasingly less validity as one goes back in time because the index is not constructed homogeneously. We also note that the u index used by SC10 uses daily means and not the local midnight values employed by IDV and we here show that equatorial u values correlate with $BV^{-0.4}$ introducing another inhomogeneity.

1.4 The m index

SC05 and SC10's IDV only uses data from any one station for 1 h during each day. However, a station will respond, to some extent, to geomagnetic activity at all UT but that response will vary with UT, giving the diurnal variation. The m index was derived by Lockwood et al. (2006b) by employing data from all hours in the day and treating each station's UT as a different station and intercalibrating each data sequence. Thus they obtained 24 times the number of data series that would be included in IDV for the same stations. Lockwood et al. (2006b) also employed the annual standard deviation for a given station at a given UT (rather than the mean interdiurnal change) and, to avoid outliers having undue influence, they used the median m rather than the mean of these data series. They also only used stations for which the data sequence extended continuously into the space age, thus minimising errors caused by "daisy chaining" a sequence of data segments. The m index is more difficult and complex in its derivation than IDV but it correlates very highly with it (correlation coefficient $r = 0.94$ for annual data after 1901). Because it is compiled in such a different manner, studying the difference between IDV and m is useful as it helps set upper limits on the uncertainties in both that are associated with their compilation procedures. However, m and IDV use much of the same historic data and so comparison of the two does not help reveal inaccuracies in those data. A point to note about m is that it employed auroral stations such as Sodankylä, and SC10 imply this invalidates its use by Lockwood et al. (2009) and Rouillard et al. (2007). However, this implied criticism is invalid because the effect of the auroral stations was to make m correlate with $BV^{0.3}$ (rather than B) and when using it Lockwood et al. (2009) and Rouillard et al. (2007) correctly employed $BV^{0.3}$ and not B.

A key point about both IDV and m is that the quality of both is necessarily lower in early years as fewer stations contribute. The effect is demonstrated by correlating IDV and m for different intervals. For 1971–2010 the average IDV is 10.38 nT, the correlation between IDV and m is $r = 0.950$, and the residuals of the best linear fit (of IDV when fitted with m) are normally distributed with a standard deviation of $\sigma_{\text{fit}} = 0.85$ nT, giving $\sigma_{\text{fit}}/<\text{IDV}> = 0.082$. Taking earlier 40 yr intervals; 1931–1970 yields $r = 0.951$ and $\sigma_{\text{fit}}/<\text{IDV}> = 0.084$ and 1891–1930 gives $r = 0.940$ and $\sigma_{\text{fit}}/<\text{IDV}> = 0.087$. Thus the quality of one or (most likely) both data series has decayed somewhat going back in time,

because of the fact that m and IDV are using largely the same sets of stations and the number of stations decreases as one goes back in time. Fewer stations means that calibration problems, site changes, and instrumental or observer error at any one site will have more effect, to the point that for just one station they will appear in full in the time series. The IDV and m indices are therefore both inhomogeneous in their derivation. This contrasts with the philosophy adopted by Mayaud (1971, 1972, 1980) in generating aa, which was to use a constant data type throughout (i.e. range data from one Northern and one Southern Hemisphere station at all times) and so generate an homogeneous sequence.

1.5 Comparing and combining indices

Both the m and the IDV indices show similar, but not identical, upward trends to aa during the 20th century. The origin of the differences will be discussed in Part 2, and here we simply note that they are different magnetic indices compiled according to distinct algorithms from different stations and so they respond to different mixtures of currents in the Earth's magnetosphere–ionosphere system. Hence we should not expect them to behave in exactly the same manner and differences in their long-term change may well be real rather than instrument or compilation error. Indeed, as first pointed out by Svalgaard et al. (2003) differences in the responses of the various geomagnetic indices to various combinations of interplanetary parameters are extremely useful as they mean that different parameters describing the near-Earth interplanetary medium can be derived using different combinations of the indices (Svalgaard and Cliver, 2007; Rouillard et al., 2007; Lockwood et al., 2009).

This paper is the first of a series of three. In it, we present a geomagnetic activity composite that is homogeneous in its construction, as far back in time as possible, using the interdiurnal variability concept. Tests are made by comparing against fully independent data that are not used in generating the composite. In Part 2 (Lockwood et al., 2013a), we use the composite to estimate the strength of the near-Earth interplanetary magnetic field (IMF) embedded in the solar wind flow since 1846. Importantly, this allows us to carry out a comprehensive analysis of errors, such the uncertainties in the composite reconstruction and those associated with the relationship between the geomagnetic activity and the IMF are both fully accounted for. We also take account of the effect of the secular change in the geomagnetic field. Part 3 is in preparation (Lockwood et al., 2013b) and will present and test a new composite of range indices, as opposed to the interdiurnal variability indices used here: this paper will also combine the two to reconstruct annual means of both solar wind speed and interplanetary magnetic field since 1845.

Table 1. Long-term and historic geomagnetic observatories employed in this study.

observatory	IAGA code	operation years	geographic latitude (° N)	geographic longitude (° E)	ht. (m)	CGM latitude in 1900 (° N)	CGM latitude in 2000 (° N)	MLT-UT in 1900 (h)	MLT-UT in 2000 (h)
Ekaterinburg	EKT	1887–1929	56.827	60.632	278	50.40	52.73	19.30	19.46
Eskdalemuir	ESK	1911–present	55.314	356.794	245	54.91	52.67	22.92	23.24
Greenwich	GRW	1840–1925	51.478	0.000	46	50.28	47.82	22.83	23.11
Hartland	HAD	1957–present	50.995	355.516	95	50.77	47.59	23.13	23.41
Helsinki	HLS	1846–1897	60.167	24.983	33	55.47	56.54	21.10	21.38
Niemegk	NGK	1931–present	52.072	12.675	78	48.53	47.95	22.03	22.29
Nurmijärvi	NUR	1953–present	60.508	24.655	105	55.86	56.91	21.11	21.39
Parc St Maur	PSM	1883–1901	48.809	2.494	50	46.92	44.39	22.73	23.00
Potsdam	NGK	1890–1907	52.380	13.060	78	48.79	48.30	22.00	22.26
Seddin	NGK	1908–1931	52.280	13.010	40	48.70	48.19	22.00	22.27
St Petersburg	SPE	1850–1862	59.933	30.300	50	54.73	56.16	20.82	21.08
Wilhelmshaven	WLH	1883–1895	53.533	8.150	10	50.85	49.81	22.27	22.55

2 Data employed

Table 1 gives details of the geomagnetic observatories employed in this study to construct a new index and to test the early variations. Figure 1 plots the variation of daily means of the horizontal field component, H, for those stations (offsets have been used to display all stations on a reduced y axis scale). Data from different stations are shown in different colours in Fig. 1. The data have been taken from various sources: data for Eskdalemuir (ESK) and Hartland (HAD) are supplied by the British Geological Survey, Edinburgh; data from Parc St Maur (PSM), Ekaterinburg (EKT) and Nurmijärvi (NUR) are available online from WDC (Word Data Centre) for Geomagnetism, Edinburgh; data from Niemegk (NGK) were supplied by H. J. Linthe of GeoForschungs Zentrum, Potsdam, Germany; data for St Petersburg (SPE) are as employed by Nevanlinna and Häkkinen (2010); data for Helsinki (HLS) are as employed by Nevanlinna (2004) and Nevanlinna and Häkkinen (2010); the Wilhelmshaven (WLH) data are taken from UCLA's Virtual Magnetospheric Observatory Data Repository where they were deposited by L. Svalgaard and E. W. Cliver. The present authors have digitised the Greenwich (GRW) data from yearbooks that were scanned and made available online by the British Geological Survey, Edinburgh. Note that the data from Helsinki and St Petersburg are not absolute values of H and a base level has been set in these cases to match model predictions. We here use the IGRF-11 model (Finlay et al., 2010) which is valid for 1900 onwards. Before then we use the gufm1 model (Jackson et al., 2000) with a smooth transition over 1890–1900 as deployed by CIRES, Boulder. For the early observatories, the long-term changes are often more due to instrument calibration drift than the secular variation in the geomagnetic field; however, the improved absolute stability of most observations after about 1880 means that most of

the changes reflect the secular variation after this date. We here show the Greenwich data uncorrected for temperature, the temperature correction being discussed later. The data labelled as NGK in fact comes from three nearby sites, Potsdam, Seddin and Niemegk itself.

Geomagnetic activity can be seen in Fig. 1 as the small (mainly downward) perturbations on short timescales ($<$ a few days). Some stations show large sudden skips in H which are caused by calibration, instrument or site changes. Apart from these shifts, the data have the same character at all stations except Greenwich, for which stability is increasingly poor between about 1890 and 1914. The Greenwich data become stable again after 1915 when completely new equipment was installed (Malin, 1996). However, urbanisation (particularly the growth of railways and tramways) were an increasing problem and after a period of overlap for intercalibration, observations ceased at Greenwich in 1926 and the data were subsequently recorded at Abinger, south of London.

As discussed above, we here adopt the approach of Mayaud (1971, 1972, 1980) to generate a homogenous data series from a small number of continuous data records, rather than to allow the number of stations used to decline as one goes back in time. Finding early, long and homogenous data series is not easy as many of the original magnetometer sites were engulfed by city growth and measurements were either closed down, moved to a new site or continued and became noisier. Inter-hour variability indices such as IHV and range k indices are the most immune to drifts in the calibration of the instrument or in the noise level as they are taken over short (3 h) intervals during which calibration shifts are generally small. Interdiurnal indices such as IDV require a bit more stability of the instrument as they require calibration and noise drifts to be small over 24 h.
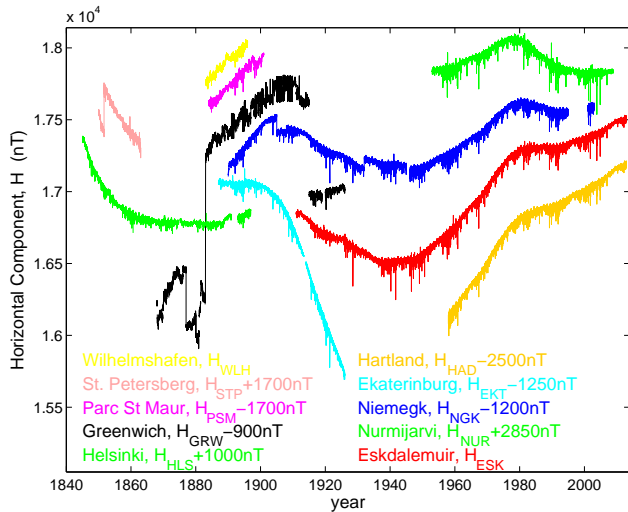
Fig. 1. Daily means of the horizontal component of the field, H, measured at the observatories listed in Table 1: red is Eskdalemuir, ESK; blue is Niemegk, NGK; green is Helsinki, HLS and (after 1952) Nurmijärvi, NUR; orange is Hartland, HAD; mauve is Parc St Maur, PSM; cyan is Ekaterinburg, EKT; black is Greenwich, GRW; yellow is Wilhelmshaven, WLH and pink is St Petersburg, SPE. Note that offsets have been introduced to reduce the y scale needed to display all the data.

The Eskdalemuir station has operated continuously since 1911, when it was established by the Kew Observatory on a rural and exceptionally clean magnetic site when the Kew site was rendered too noisy by the introduction of trams into west London (Harrison, 2004). There was a discontinuity in a commonly used set of hourly mean data from ESK (see review by Lockwood, 2013, and references therein): prior to 1932 the data stored in the WDC system were 2 h running means of the yearbook data which greatly influences inter-hour indices such as IHV. All data from ESK now available from the WDC for Geomagnetism, Edinburgh, are hourly means with no running mean smoothing applied (Macmillan and Clarke, 2011). (Users should check which data set they are using because one problem with data that has been corrupted or massaged is that it very hard to expunge from all data sets and bad data tends to resurface.) This issue illustrates very clearly and very graphically the great importance of knowing, as far as is possible, the true provenance of historic data and of all the corrections and changes that may have subsequently been applied to them (see discussion by Lockwood, 2013).

The Helsinki Observatory provides a long, continuous sequence of high-quality early data, but which does not quite overlap with ESK. It was founded in 1844 with regular data recording commencing in July that year and the observing equipment and observation methods were kept the same for almost 70 yr. We employ data for full calendar years and so use the data from 1 January 1845 onward. Observations were

taken every 10 min until 1857 after which hourly spot values were recorded. Data recording continued after 1897, but they are not hourly and installation of the Helsinki tram system generated noise which renders these data unusable for studying geomagnetic activity. The H data are not absolute but the quality of the variation data has been found to be high until 1897 (Nevanlinna, 2004).

It was our original intention to use Greenwich data to intercalibrate the HLS and ESK data series, and so we put considerable effort into digitising these data from the observatory yearbooks. However, as shown in Fig. 1, the stability of the station is very poor over the key interval. This appears to be related, at least in part, to the development of the Royal Observatory as an astronomical site and the deployment of large metal structures (such as telescope mountings). We note that Bartels (1932) drew attention to these stability problems in the Greenwich data. An additional problem is that daily means are often not given for disturbed days, instead of which the magnetogram trace is given from which mean values can be scaled. We have tried applying several correction algorithms that remove the larger calibration skips but those that are comparable to geomagnetic disturbances cannot be removed. Hence, as will be shown later in this paper, even after such data "cleaning" we found all interdiurnal variability indices from Greenwich grew progressively larger, compared to other stations, between 1891 and the full installation of completely new equipment in 1915. Hence there is an important lesson to be learned in that, although interdiurnal variation indices remove many of the instrumental, quiet diurnal variation and site effects by subtracting one day's data from the next, they are not immune to instrument and site stability effects and they tend to increase in magnitude when and where data quality is lower. From close inspection of the data summarised in Fig. 1 we consider all data listed in Table 1 to be usable except the Greenwich data between 1891 and 1914 and we treat the Greenwich data before 1891 with considerable caution. We note that Bartels (1932) also considered the Greenwich data after 1890 to be too unstable to generate an interdiurnal variation index.

Because the Greenwich data are questionable over the key interval we have deployed the intercalibrated Potsdam, Seddin and Niemegk data (hereafter collectively referred to as Niemegk, NGK) to join the ESK and HLS data sets. This combined NGK data set was also used in deriving both the IDV and m indices. We use the data from Greenwich (but only before 1891 and after 1915), Parc St Maur, Ekaterinburg, and St Petersburg and Wilhelmshaven as independent tests of the HLS–NGK–ESK composite derived. Hartland and Nurmijärvi are used only to check the consistency of the behaviour of the ESK data over the space age when comparisons with IMF data can be made. Nurmijärvi is used because it is closest to the old Helsinki site and Hartland because it is close to Greenwich. These data are also used to evaluate the quality of early data compared to modern standards.
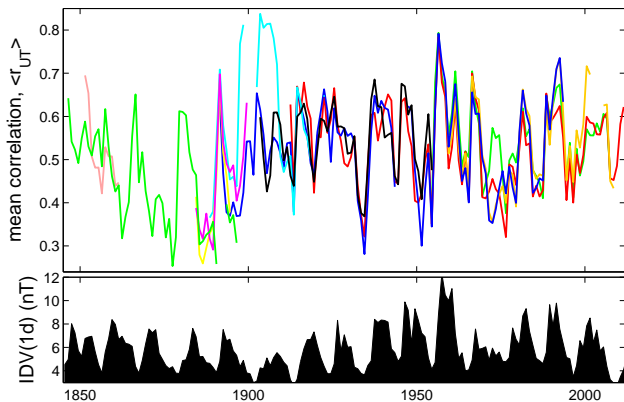
Fig. 2. (Top) The mean $<r_{UT}>$ of the 276 correlations obtained by correlating each monthly IDV(UT) time series with that for each of the other 23 UTs. The correlations are carried out over 3 yr windows (i.e. using 36 monthly means) that are incremented by 1 yr. The stations are colour-coded using the same coding as used in Fig. 1. The additional black line is for the Cheltenham magnetometer. (Bottom) Annual means of the composite IDV(1d) variation derived later in this paper.

As a test of the consistency and quality of the data used here, monthly means of interdiurnal variation were computed for each of the 24 UTs separately: IDV(UT) is defined as the absolute value of the difference in H value at a station on two successive days at a given UT. (Note that IDV(UT) for the UT closest to local midnight is SC10's IDV index.) Each IDV(UT) series for a given observatory was then correlated with each of the 23 other such series giving a total of 276 correlations per station. These were computed for 3 yr intervals (i.e. from 36 monthly values in each IDV(UT) time series), the start date of which was successively incremented by 1 yr. The mean of the 276 correlations from one station over each 3 yr interval is here termed $<r_{UT}>$. A high value of $<r_{UT}>$ reveals great similarity of the variations seen at different UTs which requires a high signal-to-noise ratio: it can decay if the signal is low and/or if the noise level is high or because geophysical conditions mean that there is increased differences between different UTs . Hence comparing simultaneous $<r_{UT}>$ values for different stations gives us an idea of their relative data quality. This test was carried out on all stations listed in Table 1 for which we have hourly data.

The results are given in Fig. 2, using the same colour scheme as Fig. 1, which shows that most of the time different stations give remarkably similar $<r_{UT}>$ values in any one 3 yr interval. The modern data (from HAD in orange, NUR in green, NGK in blue and ESK in red) give us an indication of the degree to which $<r_{UT}>$ from different stations with high quality instrumentation should agree and reveal that although there is general agreement there can be differences in the $<r_{UT}>$ values. Looking at the early data from Helsinki (HLS, in green) we do see a general decline in $<r_{UT}>$ (with large variations superposed) after 1860, and this could indi-

cate a gradual degradation in the quality of the HLS data over time (rather than a long-term change in the character of the geomagnetic activity). However, the lowest values of $<r_{UT}>$ for HLS are after 1885, by which time data are also available from PSM (mauve) and WLH (yellow) and these stations yield very similar, low $<r_{UT}>$ values at this time. Hence this minimum in $<r_{UT}>$ is geophysical in origin and does not reflect a degradation in the HLS magnetometer. By the end of the data sequence in 1897, HLS is beginning to show lower $<r_{UT}>$ than other stations which appears to be attributable to urbanisation around the site beginning to introduce noise into the data.

The one major discrepancy in the data shown in Fig. 2 is for 1897–1907 between NGK (at that time from Potsdam, in blue) and EKT (in cyan), with $<r_{UT}>$ being considerably higher for the EKT data at this time. This difference ceases in 1908 when the NGK data are taken from Seddin rather than Potsdam. This initially suggests that the Potsdam data are noisier than the EKT data. However, the large values for EKT are anomalous as they occur during solar cycle 14, which the lower panel shows to have been a very weak cycle of geomagnetic activity (the only comparably high values of $<r_{UT}>$ occurred at the peak of the strongest known cycle which is number 19). To look at this difference in greater detail we have repeated the analysis for a number of other stations that were taking data by this time and the black line shows the results for the example of Cheltenham (CLH, geographic coordinates 38.733° N, 283.158° E) which are typical. CLH, like the other stations, gives $<r_{UT}>$ very similar to those for Potsdam. We conclude that there is no problem with the Potsdam data. Bearing in mind the Eskdalemuir data change discussed earlier (Martini and Mursula, 2006; Macmillan and Clarke, 2011) we believe the most likely explanation is that the diurnal variation in the EKT data at this time may have been smoothed or may even have been recorded less often than hourly and interpolated: either would have artificially raised the r_{UT} values.

Note that this test using $<r_{UT}>$ cannot be applied to the one station about which, in Fig. 1, we have the greatest reservations, namely Greenwich. That is because before 1913, data were only recorded in the yearbooks as daily means and hourly values were not given.

3 The IDV(1d) index of geomagnetic activity

We here return to the concept of Bartels (1932) of using the mean of all data taken during a day and not just the near-midnight value (as adopted by SC05 and SC10). Hence we employ the absolute value of the difference between the daily mean values of H on two successive days. However, because we are using a single station rather than the weighted mean of a basket of stations employed by Bartels, we do not call this u, rather we adopt the terminology IDV(1d) so that it is unambiguous to what we are referring. Unlike Bartels, but

Table 2. Geomagnetic observatories compared to interplanetary conditions in this study.

observatory	IAGA code	operation years	f_{data} (%)	geographic latitude (° N)	geographic longitude (° E)	ht. (m)	CGM latitude in 2000 (° N)	MLT-UT in 2000 (h)	n_p for IDV(1d)	n_p for IDV	r_p for IDV(1d)	r_p for IDV
M'Bour	MBO	1952–present	97.07	14.380	343.030	7	0.21	0.54	–0.5	–0.2	0.897	0.889
Addis Ababa	AAE	1956–present	87.40	9.035	38.770	2441	0.75	20.95	–0.4	–0.2	0.893	0.869
Trivandrum 2	TRD	1957–1999	71.97	8.483	76.950	300	1.76	18.69	–0.6	–0.4	0.936	0.867
Guam	GUA	1957–present	95.34	13.590	144.870	140	6.19	14.73	–0.4	–0.4	0.902	0.870
Bangui	BNG	1952–2011	93.24	4.333	18.566	395	–11.00	22.21	–0.8	–0.3	0.895	0.843
Alibag	ABG	1904–present	96.56	18.638	72.872	7	16.13	18.93	–0.4	–0.2	0.897	0.864
Papeete	PPT	1966–present	90.55	–17.567	210.426	375	–16.71	8.86	–0.4	–0.1	0.904	0.889
Honolulu	HON	1961–present	94.44	21.320	202.000	4	22.32	11.13	–0.4	–0.4	0.916	0.914
Kanoya	KNY	1958–present	100	31.424	130.880	107	24.69	15.59	–0.5	–0.5	0.923	0.902
Zo-Se	SSH	1931–present	72.56	31.097	121.187	100	24.74	16.15	–0.6	–0.6	0.871	0.842
San Juan	SJG	1965–present	96.28	18.117	293.850	424	28.00	4.21	–0.4	–0.6	0.929	0.924
Kanozan	KNZ	1961–present	99.42	35.256	139.956	342	28.28	15.07	–0.5	–0.3	0.920	0.883
Antananarivo	TAN	1900–2008	72.93	–18.917	47.552	1370	–28.84	21.96	–0.4	0.2	0.836	0.757
Kakioka	KAK	1913–present	100	36.232	140.186	36	29.28	15.06	–0.4	–0.3	0.922	0.891
Tsumeb	TSU	1964–present	86.24	–19.202	17.584	1273	–30.00	23.77	–0.6	–0.2	0.859	0.833
Kandilli	ISK	1946–present	72.64	41.063	29.062	130	35.49	21.43	–0.6	0.1	0.783	0.759
L'Aquila	AQU	1960–2010	94.11	42.383	13.317	682	36.23	22.39	–0.4	0.3	0.900	0.869
Panagyurishte	PAG	1937–present	52.74	42.515	24.177	556	36.90	21.72	–0.3	0.4	0.885	0.856
Dusheti	TFS	1938–2004	80.85	42.092	44.705	980	37.42	20.49	–0.5	–0.1	0.896	0.857
Memambetsu	MMB	1950–present	100	43.910	144.189	42	37.09	14.88	–0.4	0.0	0.925	0.893
Alma Ata	AAA	1963–present	59.65	43.180	76.920	1300	38.47	18.65	–0.1	–0.4	0.883	0.842
Tucson	TUC	1909–present	95.34	32.170	249.270	946	39.77	7.74	–0.4	0.4	0.913	0.891
Hermanus	HER	1941–present	97.72	–34.425	19.226	26	–42.35	23.79	–0.5	–0.2	0.910	0.875
Fürstenfeldbruck	FUR	1939–present	97.35	48.170	11.280	572	43.36	22.45	–0.3	0.5	0.914	0.873
Chambon Le Foret	CLF	1936–present	98.78	48.025	2.260	145	43.42	23.02	–0.3	0.4	0.915	0.874
Gnangara	GNA	1957–present	93.30	–31.780	115.947	60	–44.09	16.59	–0.4	–0.2	0.893	0.862
Dourbes	DOU	1952–present	81.71	50.100	4.600	225	45.88	22.84	–0.2	0.5	0.884	0.850
Lvov	LVV	1952–present	56.61	49.900	23.750	400	45.39	21.65	–0.5	0.1	0.939	0.938
Belsk	BEL	1960–present	85.22	51.837	20.792	180	47.57	21.80	–0.2	0.4	0.927	0.897
Hartland	HAD	1957–present	99.87	50.995	355.516	95	47.59	23.41	–0.2	0.6	0.928	0.897
Irkutsk	IRT	1957–present	96.73	52.167	104.450	465	47.34	17.13	–0.3	0.1	0.919	0.898
Niemegk	NGK	1931–present	98.05	52.072	12.675	78	47.95	22.29	–0.3	0.5	0.919	0.894
Boulder	BOU	1964–present	94.77	40.140	254.767	1682	49.04	7.35	–0.4	0.3	0.912	0.912
Fredericksburg	FRD	1956–present	97.74	38.210	282.633	69	49.16	5.08	–0.4	0.2	0.912	0.926
Wingst	WNG	1939–present	98.25	53.743	9.073	50	50.01	22.49	–0.3	0.5	0.924	0.863
Novosibirsk	NVS	1967–present	94.96	54.850	83.230	130	50.54	18.26	–0.3	0.0	0.917	0.895
Krasnaya Pakhra	MOS	1930–present	70.34	55.467	37.317	200	51.42	20.77	–0.3	0.1	0.831	0.814
Brorfelde	BFE	1980–present	63.57	55.625	11.672	80	52.05	22.28	–0.1	0.7	0.909	0.781
Arti	ARS	1973–present	81.69	56.433	58.567	290	52.34	19.58	–0.2	0.2	0.893	0.850
Eskdalemuir	ESK	1911–present	99.94	55.314	356.794	245	52.67	23.24	–0.1	0.9	0.930	0.865
Victoria	VIC	1956–present	91.40	48.520	236.580	197	53.80	8.87	–0.3	0.5	0.889	0.887
Newport	NEW	1966–present	82.58	48.267	242.883	770	54.93	8.38	–0.1	0.6	0.851	0.790
Lovo	LOV	1928–2004	86.29	59.344	17.824	25	55.90	20.82	–0.1	0.6	0.879	0.772
Ottawa	OTT	1968–present	86.62	45.403	284.448	75	55.98	4.92	0.0	0.2	0.830	0.759
Voeikovo	LNN	1947–present	52.04	59.950	30.705	70	56.17	21.06	–0.1	0.4	0.867	0.808
Nurmijärvi	NUR	1953–present	97.13	60.508	24.655	105	56.91	21.39	0.0	0.6	0.879	0.841
Lerwick	LER	1923–present	97.73	60.138	358.817	85	57.99	22.97	0.1	0.7	0.902	0.890
Port Aux Francais	PAF	1957–present	92.85	–49.353	70.262	35	–58.55	20.54	0.2	0.9	0.866	0.890
Sitka	SIT	1904–present	95.88	57.067	224.670	24	59.74	9.97	0.3	1.1	0.862	0.867
Meanook	MEA	1916–present	92.62	54.616	246.653	700	62.09	8.17	0.6	0.6	0.868	0.875
Sodankylä	SOD	1946–present	93.18	67.367	26.633	178	63.92	21.06	1.0	1.5	0.921	0.877
Leirvogur	LRV	1957–present	99.63	64.183	338.300	5	65.00	0.17	0.7	2.2	0.904	0.789
College	CMO	1948–present	85.18	64.870	212.140	197	65.03	11.18	1.1	1.0	0.821	0.858
Narssarssuaq	NAQ	1968–present	71.03	61.167	314.567	4	66.19	2.14	1.0	3.8	0.833	0.761
Fort Churchill	FCC	1957–present	88.33	58.759	265.912	15	68.92	6.56	1.7	0.4	0.609	0.855
Barrow	BRW	1975–present	81.88	71.300	203.380	12	70.04	12.20	0.7	1.1	0.744	0.833
Godhavn	GDH	1975–present	92.42	69.252	306.467	15	75.70	2.43	0.5	3.3	0.914	0.829
Scott Base	SBA	1957–present	88.11	–77.850	166.763	16	–79.95	6.94	0.3	–0.3	0.787	0.477
Dumont d'Urville	DRV	1957–present	89.14	–66.667	140.007	30	–80.52	12.92	0.8	1.2	0.763	0.681
Resolute Bay	RES	1952–present	83.99	74.690	265.105	30	83.33	7.26	0.1	0.5	0.834	0.812
Qaanaaq	THL	1955–present	88.48	77.483	290.833	57	85.27	3.02	–0.1	0.9	0.869	0.806

like SC10, we use only the *H* component for both IDV(1d) and IDV, rather than the component which gives the larger value. This is because the latter option introduces a discontinuous inhomogeneity into the data and causes the latitudinal variation to become more complex. The only other data processing point to note is that values of both IDV(1d) and IDV that are more than 4 times the standard deviation are removed as a way of eliminating values caused by the calibration skips seen in Fig. 1. Because variations are smaller away from magnetic midnight, IDV(1d) is always smaller than IDV: however, the two correlate exceptionally highly (for example for HAD we find the correlation is 0.985, and for ESK it is 0.977). Nevertheless we have six reasons for making the change from IDV to IDV(1d).

1. We find that IDV(1d) correlates very slightly more highly with the IMF *B* than does IDV. (For example, annual means for Hartland IDV(1d)$_{HAD}$ give a correlation of $r = 0.912$ with annual means of *B* whereas IDV$_{HAD}$ gives 0.896; corresponding values for Eskdalemuir are 0.914 for IDV(1d)$_{ESK}$ and 0.839 for IDV$_{ESK}$.) In the next section we show this improvement is found for almost all of a basket of 91 stations studied for the modern era, which are listed in Table 2. We think the differences are because there is more information in IDV(1d) than IDV as it uses data from all 24 h in a day, rather than just one, and that this gives some noise reduction which outweighs any effect of variability in the diurnal variation.

2. The use of whole-day averages allows us to employ the yearbook data on daily means from Greenwich and other observatories to construct IDV(1d) whereas IDV can only be constructed for after 1913 for this site when the yearbooks start to record the hourly mean data.

3. Using the IGRF model we find that the UT of local midnight (computed using the online corrected geomagnetic coordinates (CGM) facility provided by NASA/Omniweb at http://omniweb.gsfc.nasa.gov/vitmo/cgm_vitmo.html) has drifted by more than 40 min since 1900 for some stations. This drift would influence IDV by shifting the average position of the substorm current wedge relative to the location of the station at the time the data used were taken. By taking daily means, IDV(1d) avoids this problem. Corrected geomagnetic coordinates are described by Gustafsson et al. (1992).

4. The effects on IDV of changing from spot values to full hourly means in the early records were found to be undetectable by SC10; nevertheless any error would be reduced further if 24 such spot values are averaged to give a daily mean.

5. The use of local midnight values only for IDV introduces a greater influence of the nightside auroral electrojet and the substorm current wedge. This additional auroral contamination introduces a changed response and a greater dependence on solar wind speed at a given latitude than is the case for IDV(1d) and means that the range of magnetic latitudes of usable stations is smaller for IDV.

6. We find that the latitudinal variation of the amplitude of IDV(1d) responses is much cleaner than for IDV. This is here used in the allowance for secular variations.

The justifications for these statements are presented in the next section.

4 Comparison of the performance of the IDV(1d) and IDV indices over the space age

The 91 stations listed in Table 2 were used to evaluate the performance of the IDV and IDV(1d) indices. For each station, annual means were formed and correlated with the product BV^n, where *B* is the near-Earth IMF field strength, *V* is the solar wind speed and *n* is an exponent that is varied between -2 and 4 (as employed by Lockwood, 2013, for a variety of geomagnetic indices). To eliminate the effect of data gaps, annual means for *B*, *V* and the geomagnetic index were constructed such that data gaps were introduced into all three if less than 75 % of the *B* or *V* data were present in the two-day interval that contributes to each index value, or if the daily index value itself were missing. Data between 1996 and 2012 were employed. The peak correlations, r_p, and the exponent *n* giving that peak correlation, n_p, are listed in Table 2 for both IDV(1d) and IDV and plotted as a function of corrected geomagnetic latitude, Λ, in Fig. 3. The lower two panels show that generally IDV(1d) is slightly but consistently more highly correlated with the interplanetary data than IDV; indeed the bottom panel shows that only in 6 of the 91 cases is the correlation higher for IDV than IDV(1d), 3 of these were at auroral latitudes. Correlations generally fall away slightly at the highest latitudes ($\Lambda > 60°$). The top panel clearly shows the effect of auroral contamination with the dependence on *V* rising to peaks at the centre of the auroral oval. For IDV(1d) the largest n_p is 2, as found by Finch et al. (2008) in the midnight auroral oval, and expected because of the effect of solar wind dynamic pressure on the substorm current wedge, as explained by Lockwood (2013). For the lowest latitudes, n_p for IDV(1d) is near -0.4 and there is a smooth variation with Λ. Note that Eskdalemuir and Nurmijärvi (red and green dots) are at ideal latitudes to remove the effects of *V* because they are clustered around the latitude where n_p goes to zero. Niemegk (blue dot) is slightly too far south of the ideal latitude (giving $n_p \approx -0.3$). On the other hand, the variation for IDV is more noisy and
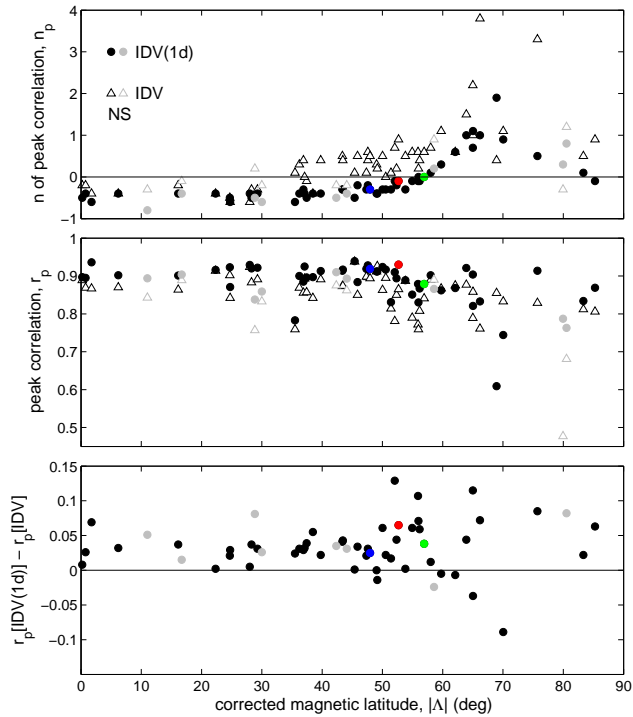
Fig. 3. Analysis of the correlations between IDV(1d) and IDV and BV^n as a function of corrected geomagnetic latitude, Λ. In all three panels, open triangles are for IDV, filled circles are for IDV(1d) and black and grey for the Northern and Southern (magnetic) Hemisphere stations, respectively. Results for Eskdalemuir, Neimegk and Nurmijarvi are shown in red, blue and green dots, respectively. (Top) The exponent of V giving the peak correlation, n_p; (middle) the peak correlation coefficient, r_p; and (bottom) the difference between r_p for IDV(1d) and IDV.

Fig. 4. Analysis of IDV(1d) variations with station corrected geomagnetic latitude. (Top) The ratio $f_X = <\mathrm{IDV(1d)}_{\mathrm{ESK}}/\mathrm{IDV(1d)}_X>$; (bottom) the correlation with Eskdalemuir data, r_E. The dashed line in the upper panel is the $\cos(\Lambda_X)$ variation employed by Bartels, the dot-dash line is the $\cos^{0.7}(\Lambda_X)$ variation employed for IDV by SC05 and the solid line is a seventh-order polynomial weighted fit given by Eq. (1).

n_p is about -0.2 at the lowest latitudes, passes though zero around $\Lambda = 30°$ and shows some very large values in the auroral oval. Even for a station at as low a latitude as Niemegk $n_p \approx 0.5$ and for Eskdalemuir it is 0.9. Hence the auroral contamination, giving increased dependence on V, is reaching to lower Λ in the case of IDV, due to the use of near-midnight values, closer to the substorm current wedge. SC10 employ IDV data from Eskdalemuir (which depends on $BV^{0.9}$) but not Nurmijärvi (which depends on $BV^{0.5}$) in a composite index that, on average, depends on $BV^{-0.1}$ in the space age. Using a variable mix of all station data that is available means that we do not know what the n_p value for the composite index before the space age was.

Figure 4 shows another study of the latitudinal properties of IDV(1d), again over the 1966–2012 interval. The lower panel shows r_E, the correlations between the data series for each station and the Eskdalemuir data series. The vertical dashed line is the peak Λ used in the composite derived here (at any epoch). At latitudes below this the correlations are over 0.96. Poleward of this latitude, r_E falls because the auroral contamination (and consequent dependence on V) be-

comes a factor. By definition, r_E is unity for Eskdalemuir but values are high for Niemegk and Nurmijärvi (0.99 and 0.98, respectively). The upper panel in Fig. 4 shows the average ratio of the Eskdalemuir IDV(1d) index, IDV(1d)$_{\mathrm{ESK}}$, and that at each other station (at latitude Λ_X), IDV(1d)$_X$. This is computed by taking the ratio for each day (when both are available) and then taking the mean of that ratio for the whole 46 yr interval. As expected from Bartels' u index, the ratio $f = <\mathrm{IDV(1d)}_{\mathrm{ESK}}/\mathrm{IDV(1d)}_X>$ falls at lower Λ. The dashed line shows the variation that would be predicted from the $\cos(\Lambda_X)$ variation employed by Bartels, whereas the dot-dash line is the $\cos^{0.7}(\Lambda_X)$ variation employed for IDV by SC05. The solid line is a seventh-order polynomial fit, constrained to pass through the normalising Eskdalemuir data point and with points weighted by r_E^2, given by

$$
\begin{aligned}
f_X =&< \mathrm{IDV(1d)}_{\mathrm{ESK}}/\mathrm{IDV(1d)}_X >= -3.818 \times 10^{-13}\Lambda_X^7 \\
&-3.141 \times 10^{-11}\Lambda_X^6 + 1.958 \times 10^{-9}\Lambda_X^5 \\
&+1.340 \times 10^{-7}\Lambda_X^4 - 1.989 \times 10^{-6}\Lambda_X^3 + 9.520 \\
&\times 10^{-2}\Lambda_X^2 + 5.460 \times 10^{-4}\Lambda_X + 0.534.
\end{aligned}
\tag{1}
$$

The advantage of this polynomial fit is it accurately reproduces the flatness of the curve in between the latitudes of the Eskdalemuir, Niemegk and Nurmijärvi stations. Note the spread of f_X values at subauroral latitudes; we find that this spread is associated with both the longitude of the station and the magnitude of the local field. Hence when constructing a homogeneous index we need to make sure that variations in these, as well as in the station latitude, are kept as constant as possible. By using a weighting of r_E^2, the polynomial given by Eq. (1) fits the stations best that correlate well with Eskdalemuir (which generally are nearby).

Figure 5 shows the plot corresponding to Fig. 4 for IDV, normalised to Niemegk (as used by SC05). We note two factors. Firstly, the latitudinal variations of both f_X and r_E are similar to those for IDV(1d) but are considerably noisier. Secondly, the auroral contamination spreads to lower latitudes, as already seen in Fig. 3. This is particularly demonstrated for the behaviour of IDV_{NUR} (the green dots in Fig. 5) for which both r_E and, in particular, f_X are reduced. The key point is that Fig. 5 shows that for the Nurmijärvi station, auroral contamination is a serious problem for IDV but Fig. 4 shows that it is not a problem for IDV(1d) from this station. This is important for the IDV(1d) composite reconstruction presented here because Nurmijärvi is close to the old Helsinki Observatory and so we can use the early data from that station provided that 1 d means (i.e. $IDV(1d)_{HLS}$) are used rather than near-midnight values (i.e. IDV_{HLS}) because the averaging reduces the auroral contamination and provides noise suppression by averaging.

5 Construction of the HLS–NGK–ESK composite

5.1 Joining the HLS and NGK data

The biggest difficulty in the construction of the composite was in joining the HLS and NGK data sets. This is because the overlap interval is relatively short (1890–1897) in full data and HLS data are missing in 1891 and 1892. Fortunately, the overlap interval does cover much of the rising and falling phases of a reasonably large-amplitude solar cycle (cycle number 13) and so there is a reasonable dynamic range to correlate on. The correlation is carried out on means over 27 d Bartels rotation intervals and daily means are excluded from one station if there is a data gap in the data series from the other to avoid such gaps influencing the correlation (Finch and Lockwood, 2007). This yields 80 pairs of 27 d means which gave a correlation coefficient of 0.818.

Figure 6 shows the scatter plot and regression fits of the Bartels rotation means of $IDV(1d)_{NGK}$ and $IDV(1d)_{HLS}$ using ordinary least squares (OLS) regression. The regression slope was found to be somewhat different if least median squares (LMS) or Bayesian least squares (BLS) were used (Lockwood et al., 2006a, and references therein), but the procedures converged on very similar regression lines if outliers
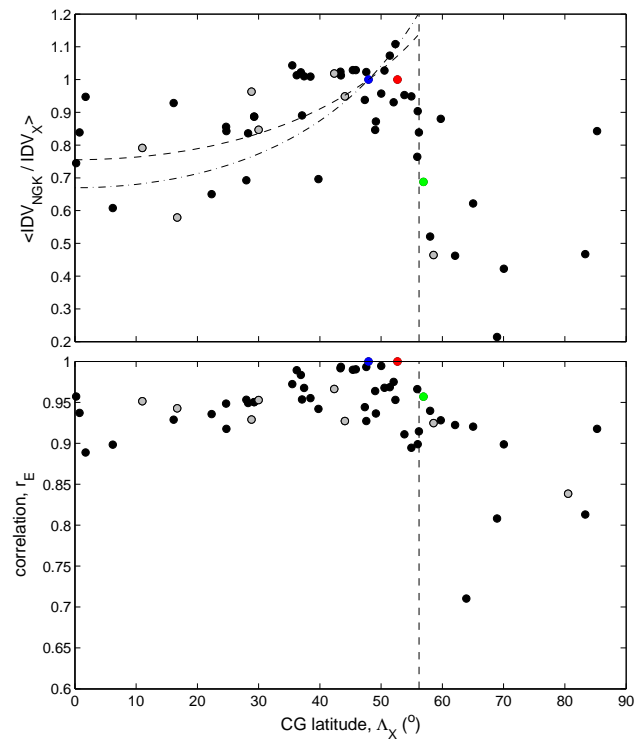

Fig. 5. Analysis of IDV variations with station corrected geomagnetic latitude in the same format as Fig. 4. (Top) the ratio $f_X = \langle IDV_{NGK}/IDV_X \rangle$; (bottom) the correlation with Eskdalemuir data, r_E.

were progressively removed. Hence we here use OLS but the largest outliers were removed until the regression converged on a stable line. These outliers usually had the largest Cook-D leverage factors and so the regression slope tended to oscillate to its optimum value as the outliers were removed. Commonly used equations for the errors in linear regression are not generally adequate (Richter, 1995) and because the regression is most influenced by large-leverage outliers, uncertainties are here set conservatively (i.e. potentially overestimated) by taking the largest and smallest linear regression values obtained during the successive removal of the largest outliers between $N_r = 0$ and $N_r = 8$ (which is 10 % of the available data). Figure 3 identifies the outliers (each determined after regression re-fitting following removal of the previous outlier) by showing them as coloured points that were removed in the order red, orange, yellow, green, cyan, blue, mauve, and then grey: the black line is the regression for no outlier removal and the red line the regression after the red point was removed, and so on. The correlation coefficient prior to removals was $r = 0.818$. The regression was considered not greatly influenced by outliers after $N_r = 4$ outliers were removed out of the total of 80 available data points.

The authors anticipate that some scientists who do not appreciate the pitfalls of least squares regression will argue that the removal of the outliers is arbitrary and has influenced the
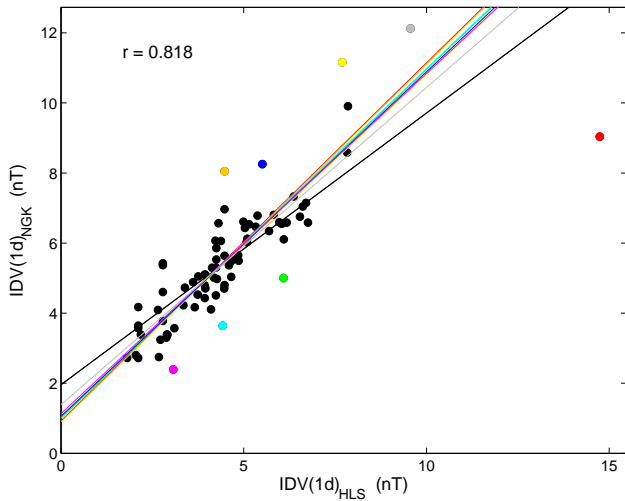
Fig. 6. Scatter plot of Bartels rotation interval means of IDV(1d) values from Helsinki and Niemegk, IDV(1d)$_{HLS}$ and IDV(1d)$_{NGK}$ respectively, for 1890–1897. The coloured dots show outliers removed in the order red, orange, yellow, green, cyan, blue, mauve, and grey. The black line is the regression for no outlier removal and the red line the regression after removal of the red point, and so on. The regression was considered not greatly influenced by outliers after $N_r = 4$ outliers were removed out of the total of 80 available data points. The correlation coefficient prior to removals was $r = 0.818$.
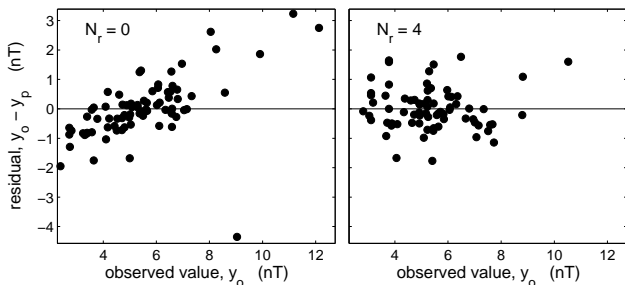
Fig. 7. Fit residuals for two of the regression fits shown in Fig. 6, after N_r outliers have been removed following re-fitting for (left) $N_r = 0$ and (right) $N_r = 4$. The observed value, y_o, is here the 27 d NGK data that we are matching the HLS data to, the predicted value, y_p, is the HLS data, scaled by the regression fit, hence $(y_o, -y_p)$ is the fit residual.

results. Figures 7 and 8 show why their removal is essential and that the fit obtained without removing them is both biased and violates the principles of OLS regression. Figure 7 shows the fit residuals as a function of the NGK data that we are fitting the HLS data to. It can be seen that for no removal of outliers ($N_r = 0$) the fit shows a consistent trend in the fit residuals such that when IDV(1d)$_{NGK}$ is large the fit to it using IDV(1d)$_{HLS}$ is consistently an underestimate, whereas when IDV(1d)$_{NGK}$ is small the fitted value is consistently an overestimate. The right hand plot shows this problem has been solved by the removal of $N_r = 4$ outliers and
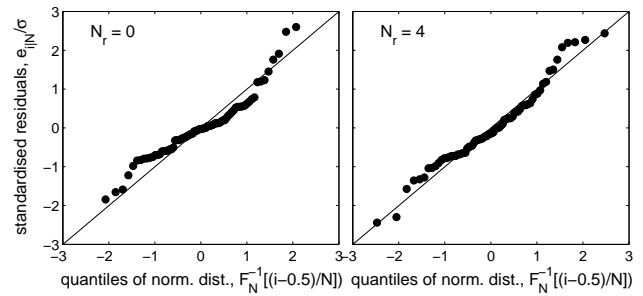

Fig. 8. "Q-Q plots" for two of the regression fits shown in Figs. 6 and 7, after N_r outliers have been removed following re-fitting for (left) $N_r = 0$ and (right) $N_r = 4$. The ordered, standardised fit residuals $(y_o - y_p)/\sigma$ (where σ^2 is $\Sigma_{i=1}^{n}(y_o - y_p)_i/(n-2)$ and n is the number of samples) are shown as a function of the corresponding quantiles of a standard normal distribution.

neither the mean nor the spread of the fit any longer shows a trend in the fit residuals (Lockwood et al., 2006a; Lockwood, 2013). Figure 8 shows a second test of these two fits. This figure shows the "Q-Q plots" in which deviations from the shown line of unity slope reveal departures from a normal distribution of residuals, which is assumed by the theory of least squares fitting (Wilks, 1995; van Storch and Zwiers, 1999). Figure 8a shows that for $N_r = 0$ the distribution is not Gaussian but Fig. 8b shows that removing the 4 worst outliers has made the bulk of the residual population normally distributed. (Both tails of the distribution still show departures from a Gaussian and these are only marginally decreased by removal of further outliers and make little difference to the regression fit.) We have checked that all regressions used in this paper pass these tests for bias, homoskedasticity and a normal distribution of residuals. The example discussed here is the lowest correlation coefficient of any used in this paper and in Parts 2 and 3; the importance of the tests and the effect of removing outliers are both lower for all other regressions, because the associated correlation is higher.

Using the regression for $N_r = 4$, the 27 d IDV(1d)$_{HLS}$ data are re-scaled and appended to the start of the NGK data, giving a composite of the HLS and NGK data sets. The re-scaled HLS data are used where available, but data gaps in that sequence are filled using the NGK data. The uncertainty is set by the full range of the effect of removing the top 8 outliers. Tests of this joining of the HLS and NGK data will be made later in this paper using fully independent data from different stations in the European sector.

5.2 Joining the NGK/HLS composite to ESK data

The NGK/HLS data composite is then re-scaled in the same way and appended to the start of the ESK data. The scatter plot corresponding to Fig. 6 is shown in Fig. 9. Although the correlation was higher (correlation 0.932 before the removal of outliers from the 123 pairs of 27 d means), in this case
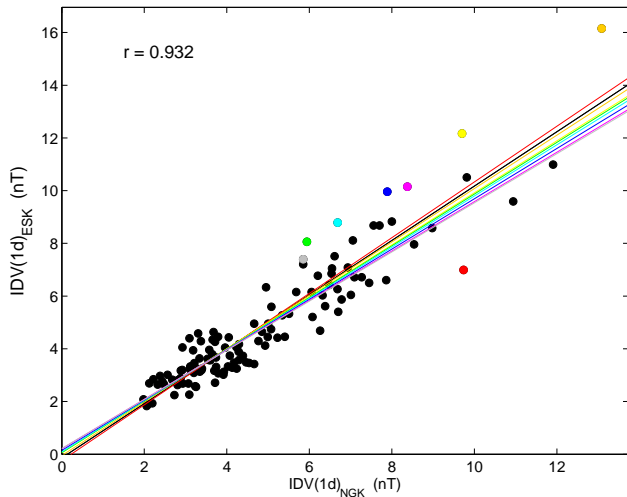
Fig. 9. Scatter plot of Bartels rotation means of IDV(1d) values from Niemegk and Eskdalemuir for 1911–1920, IDV(1d)$_{NGK}$ and IDV(1d)$_{ESK}$ respectively, shown using the same format as Fig. 3. The regression was considered not greatly influenced by outliers, and the plot residuals rendered homoskedastic and normally distributed after $N_r = 8$ outliers were removed out of the total of 123 data points. The correlation coefficient prior to outlier removals was $r = 0.932$.

the removal of outliers did not cause the fit to converge as rapidly because, as shown in Fig. 9, most of the largest $N_r = 8$ outliers lay above the regression fits. However, increasing N_r further did not change the slope further nor did it further improve the distribution of residuals. One point to note is that this correlation was taken over the interval between the start of the ESK data (1911) and 1920. This upper date could have been chosen to be later as both the data sets continue after it. However, it must be remembered the point of the exercise is to fit the two sequences together at 1911 and discrepancies in later data (for example the different effect of the secular drift on the two stations) could start to introduce a discontinuity at the join. The upper limit to the date range was increased (giving more samples) until there was a detectable effect on the join. The date of 1920 was chosen as the upper limit at which there was no detectable effect.

5.3 The complete composite and allowing for the secular field change

Using the two regressions discussed in the previous two subsections, a single composite data sequence was generated. This would be the final composite, however there is a final correction to make first. The secular change in the geomagnetic field means that the magnetic latitude of the stations has drifted with time. Figure 10a shows the predicted CGM (Gustafsson et al., 1992) latitude, $\Lambda_{[X,d]}$, of station X at a date d. These latitudes are computed from the IGRF-11 model as a function of d between 1900 and 2015. Red is for
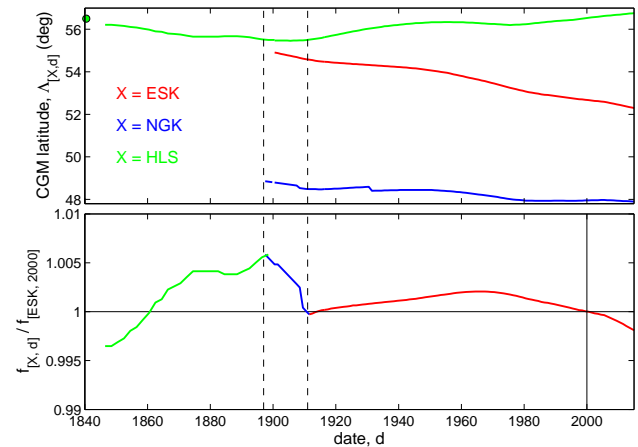

Fig. 10. (Top) The variation of the corrected geomagnetic latitude of ESK (red), NGK (blue) and HLS (green) as a function of date, d. After 1900 values are from the IGRF model (Finlay et al., 2010); before then they are from the gufm1 model (Jackson et al., 2000) with a smooth transition in value and slope implemented over 1890–1900. The green point is the estimate of $\Lambda_{[HLS,1840]}$ of 56.50° from Nevanlinna (2006). The small discontinuities in the $\Lambda_{[NGK]}$ curve at 1907 and 1931 arise from the moves of the NGK station from Potsdam to Seddin and from Seddin to Niemegk. The blue curve has been extrapolated back to 1897 from 1900 using cubic splines on $\Lambda_{[NGK]}$ for the Seddin site (used for 1897-1907 in the composite). (Bottom) The composited IDV(1d) correction factor to normalise the composite for contributing station (X) on a given date (d) to ESK in the year 2000, $f_{[X,d]}/f_{[ESK,2000]}$.

ESK, blue for NGK and green for HLS. The IGRF model cannot be used before 1900, and we need to know the CGM latitude of the HLS and NGK stations before then. As before we use the gufm1 model. By way of comparison, the green dot shows corrected magnetic latitude of HLS for 1840 of $\Lambda_{[HLS,1840]} = 56.50°$ N, derived by Nevanlinna (2006) using the first three spherical harmonic coefficients for the older historic field model by Barraclough (1978; see also Barraclough, 1974). For NGK we need to extrapolate only back to 1897, just 3 yr before 1900 (when IGRF-11 can be applied). The small dashed segment of the blue line is an extrapolation of $\Lambda_{[NGK]}$ for Seddin using cubic splines.

To look at the consequences of these shifts in station geomagnetic latitude, we here make use of the dependence of IDV(1d) from the European sector on corrected geomagnetic latitude given by Eq. (1). We normalise to ESK in the year 2000 (so that it will be relatively straightforward to update the data sequence using future ESK data), so normalised data are given by

$$\text{IDV(1d)} = \text{IDV(1d)}_{[X,d]} \times f_{[X,d]}/f_{[ESK,2000]}. \qquad (2)$$

Figure 10 shows the factor needed to normalise the contributing station (X) at a given date d to the ESK in the year 2000, $f_{[X,d]}/f_{[ESK,2000]}$, computed from the $\Lambda_{[X,d]}$ shown in the upper panel. These sequences have been splined together
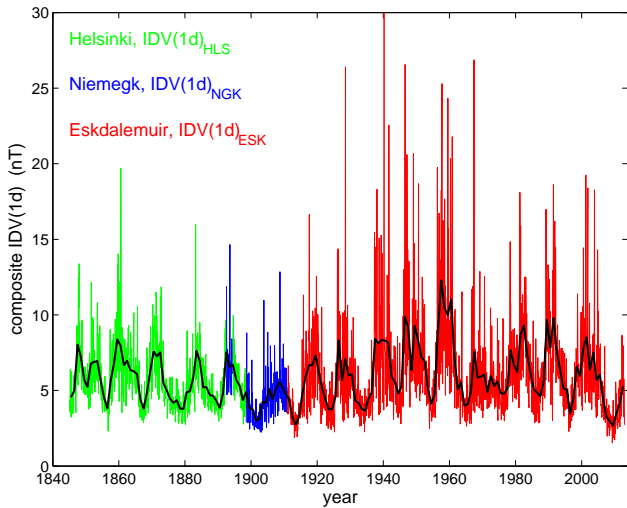
Fig. 11. The composite variation (normalised to the Eskdalemuir site in 2000 using the station-latitude correction factor shown in Fig. 10, bottom panel). The coloured lines show 27 d Bartels rotation means (red for data originating from ESK, blue for NGK and green from HLS), and the black line shows annual means.

Fig. 12. Scatter plot of annual means of the IDV(1d) composite, shown in Fig. 8, as a function of the IDV index, as derived by SC10, against those for 1880–2013, using the same format as Fig. 3. The correlation coefficient is $r = 0.957$ and removing outliers makes almost no difference to the regression fit because the correlation coefficient is so high. The best-fit regression slope is $s = 0.678$ and the intercept is $c = -0.765$ nT.

using the regression coefficients found in Sects. 5.1 and 5.2, such that the full sequence can be applied to the intercalibrated HLS–NGK–ESK composite. By definition the factor is unity in 2000 and between 1840 and 2015 it is within 0.5 % of this value at all times. The motion of the geomagnetic pole has been such that the correction for the stations chosen is very small. Nevertheless is has been quantified and implemented.

There is a somewhat circular argument to this correction, in that the model fields used to generate the correction factor is derived from a fit to magnetometer data, including that from the stations that we are here trying to find the magnetic latitude for. However, application of this correction does remove the possibility that any long-term drift in the composite is due to any special location(s) of the station(s) that happen to have been used to construct it. This is confirmed by the very high correlation and almost identical long-term drift (see below) found when comparing the corrected IDV(1d) composite and the IDV index for the past 130 yr, when many stations from all round the globe have been used to generate IDV.

Figure 11 shows the final composite, normalised to the Eskdalemuir site in 2000 using the correction factor shown in the bottom panel of Fig. 10. The coloured lines show 27 d Bartels rotation means (red for data originating from ESK, blue from NGK and green from HLS), the black line shows annual means. Figure 12 shows the scatter plot of annual means of the IDV(1d) composite as a function of the IDV index, as derived using many stations by SC10. This plot is for data after 1880 and it can be seen that the agreement is excellent. Figure 13 uses the best-fit regression to scale IDV
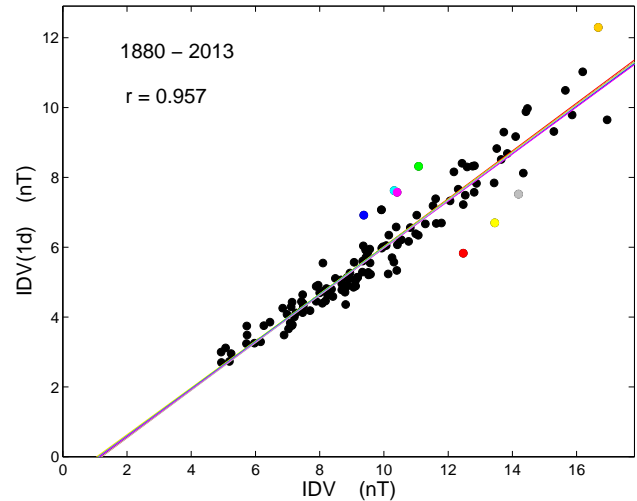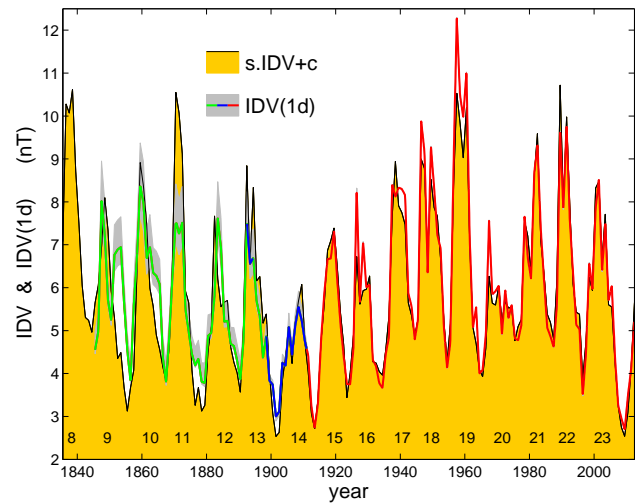

Fig. 13. Annual means of the IDV(1d) composite, with data originating from ESK in red, NGK in blue and HLS in green. The black line bounding the filled orange area is the IDV index of SC10, scaled using the regression for 1880–2013, as shown in Fig. 9. The grey area shown is the band of uncertainty that arises from the two regression fits used to compile the composite (so between 1890 and 1911 the uncertainty arises from the NGK–ESK regression and before 1890 it arises from both the NGK–ESK and the HLS–NGK regressions). Solar cycle numbers are given across the base of the plot.

onto a plot of the time series of the IDV(1d) composite. Also shown, as a grey band, is the combined uncertainty arising from the two regressions used to join the data sets together into a composite. The exceptional agreement between the IDV(1d) composite and IDV after 1880 is apparent. Note that this means that the scaled HLS data of our composite agrees very well with IDV for most of two solar cycles (cycles 12 and 13, 1880–1897). However, before 1880 the agreement is quite poor. In particular, IDV shows some large amplitude cycles that are not seen in the scaled HLS data (particularly cycle 11). The annual means of the IDV(1d) composite and its uncertainty are given in Table 1 of Part 2 (Lockwood et al., 2013a).

6 Comparison with other data

Figure 14 is a detailed view of Fig. 13 for before 1930. It also shows annual mean IDV(1d) data from the other observatories listed in Table 1. In each case, the data are normalised to Eskdalemuir in 2000 using Eqs. (1) and (2) so as to remove the effects of the secular change in the field. All the data agree well with the IDV(1d) composite, which is significant as none of them contributed to the composite and so form independent tests. The Ekaterinburg data $IDV(1d)_{EKA}$ cover both joins in the composite and agree well over solar cycles 13, 14 and 15. Similarly, the Parc St Maur data $IDV(1d)_{PSM}$ agree well with both the new composite and the IDV variation.

The Greenwich data, $IDV(1d)_{GRW}$, require some explanation and are the least reliable of the data shown. The measurement of the H component requires a temperature correction and for many of the Greenwich Observatory yearbooks this means that both the uncorrected values and the equipment temperature data must be digitised and the temperature correction correctly implemented. In addition, for many of the years mean values are not given for disturbed days (instead plates of the magnetogram traces are given). Fortunately, for 1882–1911 the yearbooks give both the corrected and uncorrected values in the same table and using these data the effect of the temperature and of the missing days on the annual mean $IDV(1d)_{GRW}$ values can be evaluated. Of these years, data for 1892 and after are not usable because of the data stability issues seen in Fig. 1. From the remaining 10 yr we find that the corrected values give annual means of $IDV(1d)_{GRW}$ that are, on average, 0.94 times the values obtained from uncorrected data. The largest value of this ratio is 1.02 and the smallest 0.86. Hence we here apply a factor of 0.94 ± 0.08 to allow for the temperature effect and the effect of missing days, giving the error bars shown in Fig. 14. Between 1893 and 1914, the Greenwich data appear to us to be unusable because of the stability effects noted in Fig. 1. The small dots in Fig. 14 show the values of $IDV(1d)_{GRW}$ derived in these years after an attempt was made to clean the H data. This was done by identifying all the daily $IDV(1d)_{GRW}$
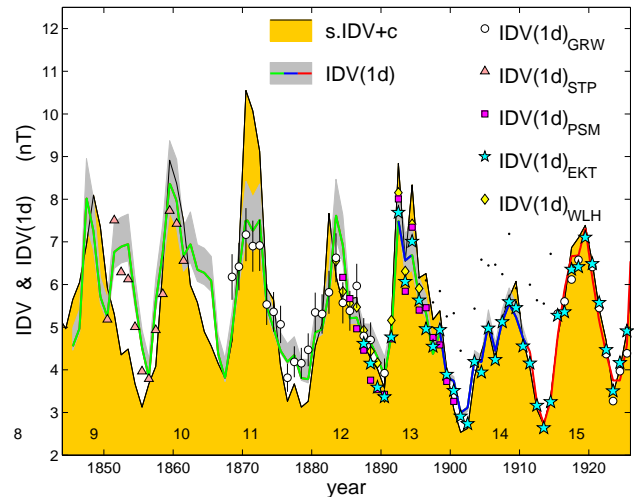

Fig. 14. Detail of Fig. 13 for before 1930. Annual means of the IDV(1d) composite are shown with data originating from ESK in red, NGK in blue and HLS in green, surrounded by a grey area showing the band of uncertainty that arises from the two regression fits. The black line bounding the filled orange area is the IDV index of SC10, scaled using the regression for 1880–2013, as shown in Fig. 12. IDV(1d) derived from various early data sets are also shown: from St Petersburg, $IDV(1d)_{SPE}$ (pink triangles); from Ekaterinburg, $IDV(1d)_{EKA}$ (cyan stars); from Parc St Maur, $IDV(1d)_{PSM}$ (mauve squares); from Wilhelmshaven, $IDV(1d)_{WLH}$ (yellow diamonds); and from Greenwich, $IDV(1d)_{GRW}$ with σ_H < 30 nT (white circles). The Greenwich values are compiled using the daily means of H that are uncorrected for temperature variations, but then the annual IDV(1d) values are corrected (giving the shown uncertainty bands caused by the temperature effects). The small black dots are Greenwich data which have been cleaned to try to remove the instrumental fluctuations in H shown in Fig. 1, but which are not regarded as reliable because even after such cleaning $\sigma_H \geq 30$ nT. Solar cycle numbers are shown across the base of the figure.

values that exceeded 100 nT and then studying the variation of H around it and rejecting the data if there was a step-like change in H that indicates a calibration shift. The results gave $IDV(1d)_{GRW}$ values that show the solar cycle variation but progressively increased between 1893 and 1914 relative to the IDV(1d) composite, the IDV index and IDV(1d) values from EKT, PSM and WLH. This error is not eliminated until the new instrumentation became fully operational at Greenwich in 1915. We found intervals of concern could be identified using the standard deviation over a year of the H values, σ_H, in that $IDV(1d)_{GRW}$ begins to deviate from the other values if σ_H exceeded a threshold of 30 nT. In Fig. 14, $IDV(1d)_{GRW}$ values for $\sigma_H < 30$ nT are shown by white circles whereas those for $\sigma_H \geq 30$ nT (even after cleaning the data to try to remove stability problems) are shown by small black dots.

The St Petersburg data $IDV(1d)_{SPE}$ are much closer to the IDV(1d) composite than SC10's IDV in solar cycles 9 and

10 (before 1865). Very similar results are obtained using data from the other early Russian stations Nertchinsk (NER) and Barnaul (BAR) (Nevanlinna and Häkkinen, 2010). There are also data at this time from Ekaterinburg. However, as for the Greenwich data for 1893–1914 there are stability problems in the H data series in that $\sigma_H \geq 30$ nT for several of the years and the IDV(1d)$_\text{EKA}$ values are higher than IDV(1d)$_\text{SPE}$, IDV(1d)$_\text{BAR}$ and IDV(1d)$_\text{NER}$. Within the uncertainty error bars, the Greenwich data agree with the IDV(1d) composite but not with the IDV series: however given the several concerns about the Greenwich data, we consider this comparison indicative rather than definitive.

7 Correlations of monthly data

From the last section, the IDV(1d) composite derived here is very similar indeed to the IDV index, compiled from many stations, after about 1880. However, before 1880 there are considerable differences. At this time the composite is derived from the Helsinki magnetometer data. On the other hand, at this time IDV is the linearly regressed u index, which, before the introduction of data from Batavia in 1884, was derived from data from two stations: Greenwich and Bombay. Before 1872, u is constructed from proxy relationships to diurnal variation in declination observed at Greenwich at fixed hours of the day (termed E) and from the summed deviation from its mean of the diurnal variation of H detected at the Colaba Observatory, Bombay (termed s) (Bartels, 1932; Svalgaard and Cliver, 2010). The s and E data are fitted to the genuine u index data for between 1872 and about 1905 and the regression used to construct a proxy u for before 1872. Hence it becomes particularly important to assess the accuracy of the u data for 1872–1905.

It is very difficult to establish which of the two sequences is in error (or if both are), with so little and inadequate data to test them against. Of the two, the Helsinki data is by far the most homogeneous in its derivation, using the same procedures on the same equipment at the same site throughout. In contrast, the u index sequence contains major changes in its construction at both 1872 and 1884. Because we have hourly data from Helsinki we can test it through its $\langle r_\text{UT} \rangle$ value: Fig. 2 shows that it behaves in a similar way to other stations when comparable data are available. We cannot apply the same test to u as we have only monthly values.

It is illuminating to look at the coherence of modern data at different sites for monthly averaging timescales and compare it with the corresponding behaviour of the early data as we go back in time. The lower panel in Fig. 15 shows monthly means of the IDV(1d) from Eskdalemuir, Nurmijärvi and Hartland over a 27 yr interval (1981–2008). The Nurmijärvi Observatory has been chosen here as it is the modern station closest to the Helsinki Observatory which is used to compile the composite. The degree of correspondence between the three time series is extremely high, with an overall cor-
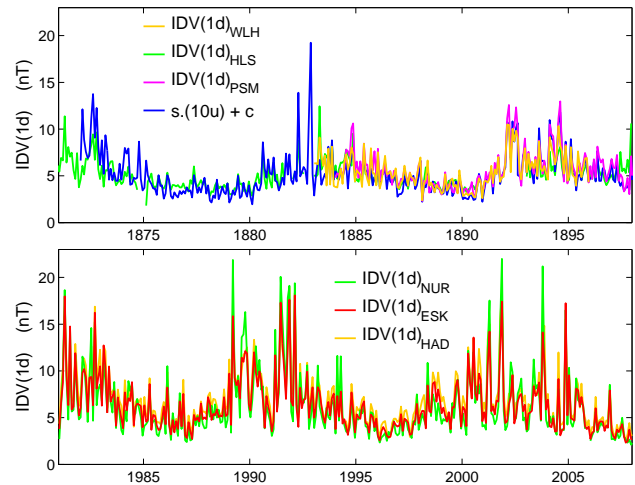

Fig. 15. Monthly means of IDV(1d) from various sources. The upper panel shows early data (1871–1898) and the lower panel an interval of modern data of the same duration (1981–2008). The upper panel shows data from Parc St Maur, IDV(1d)$_\text{PSM}$ (in mauve), from Wilhelmshaven, IDV(1d)$_\text{WLH}$ (in orange), and from Helsinki, IDV(1d)$_\text{HLS}$ (in green), along with the scaled u index, $s \cdot (10u) + c$ where s and c are given by the regression shown in Fig. 9 (in blue). (Note that the IDV $= 10u$ at this time). The lower panel shows data from Eskdalemuir, IDV(1d)$_\text{ESK}$ (in red), Nurmijärvi, IDV(1d)$_\text{NUR}$ (in green) and Hartland (in orange).

relation of 0.931 between NUR and ESK and 0.974 between HAD and ESK for these 27 d means. Taking correlations over 3 yr intervals, and incrementing the start of those intervals by 1 yr, yields 25 correlation coefficients between the NUR and ESK data, r_EN. The mean of these 25 r_EN values, $\langle r_\text{EN} \rangle$ is 0.906 with a standard deviation of $\sigma_\text{EN} = 0.042$. There is no temporal trend in the r_EN values. This high level of agreement is achieved because the observations at both Eskdalemuir and Nurmijärvi are made to the very high standards of modern observatories. Ideally, we would wish the early data to match up to this standard.

The upper panel in Fig. 15 shows early IDV(1d) data, also for a 27 yr interval (1871–1898), from Helsinki (in green), Parc St Maur (in mauve), Wilhelmshaven (in orange), along with the scaled u index, $s \cdot (10u) + c$, where the regression constants s and c are given by the linear fit shown in Fig. 12. It can be seen that there is still considerable agreement, but the correspondence is not as exact as for the modern data in the lower panel of the figure.

To quantify this, we here take correlation coefficients between the data series over 3 yr intervals (incrementing the start dates by a year) for the pairs of observatories, using the same procedure described above to derive r_EN for the modern ESK and NUR data. The results are shown in the upper panel in Fig. 16. For comparison, the horizontal black line shows $\langle r_\text{EN} \rangle$ from the NUR and ESK correlations described above and the grey band around it shows $\langle r_\text{EN} \rangle \pm 2\sigma_\text{EN}$. The
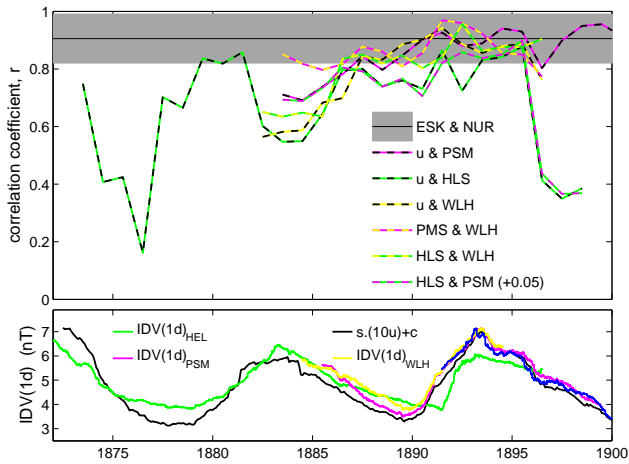
Fig. 16. (Top) Correlation coefficients, r, in 3 yr windows of monthly data: (black and green dashed line) u and IDV(1d)$_{HLS}$; (black and mauve) u and IDV(1d)$_{PSM}$; (black and yellow) u and IDV(1d)$_{WLH}$; (mauve and yellow) IDV(1d)$_{PSM}$ and IDV(1d)$_{WLH}$; (green and yellow) IDV(1d)$_{HLS}$ and IDV(1d)$_{WLH}$; (green and mauve) IDV(1d)$_{PSM}$ and IDV(1d)$_{HLS}$. The last line has been shifted up by 0.05 (approximately a line width) to avoid it sitting on top of other lines. The black horizontal line is the mean $<r_{EN}>$ for the modern data shown in Fig. 15, r_{EN} being the correlation coefficient between IDV(1d)$_{ESK}$ and IDV(1d)$_{NUR}$ in 3 yr windows between 1981 and 2008, and is surrounded by a grey band $2\sigma_{EN}$ wide, where σ_{EN} is the standard deviation of the r_{EN} values. (Bottom) 36-point (3 yr) running means over the same interval of (green) IDV(1d)$_{HLS}$; (mauve) IDV(1d)$_{PSM}$; (yellow) IDV(1d)$_{WLH}$; (blue) IDV(1d)$_{NGK}$; and (black) the scaled u index, $s \cdot (10u) + c$, where s and c are given by the regression shown in Fig. 12. Note that all IDV(1d) values used or shown here are as derived from published station H values with no re-calibrations.

pairs of colours of the dashed lines match the colour coding used in Figs. 1 and 2 (green for HLS, mauve for PSM, yellow for WLH) while blue is used for u. Hence the mauve and yellow dashed line is the correlation between PSM and WLH, the green/yellow dashed line is for the pairing of HLS and WHL, and so on. The lower panel in Fig. 16 shows 3 yr running means of the daily data, also using the same colour coding scheme.

The PSM and WLH correlation (mauve/yellow line) remains within, or very close to, the $<r_{EN}> \pm 2\sigma_{EN}$ grey band at all times. Hence these two stations show a coherence in their data series that matches that of modern data and implying that they match modern standards of accuracy on the monthly timescales studied. Between 1886 and 1896, the same is true for the correlations between WLH and u (yellow/blue dashed line) and WLH and HLS (yellow/green dashed line). Hence we can have great confidence in both u and the HLS data at this time. (Figure 16 confirms that the quality of the HLS data falls after 1896 due to the increased noise at the site as the correlations of HLS with both PSM and WLH fall.) This agrees with the behaviour

of the annual means shown in Fig. 11, in that IDV (based on u) and the composite (based on IDV(1d)$_{HLS}$) agree very closely after about 1886. However, before 1886 the correlations of IDV(1d)$_{WLH}$ with u and IDV(1d)$_{HLS}$ both decline as we go back in time, such that they are notably lower than the range for the modern data. Given that the correlation between IDV(1d)$_{WLH}$ and IDV(1d)$_{PSM}$ remains at high levels, this strongly implies that both the u index and HLS data decline in accuracy as we move back in time from 1886. The similarity of the declines in the correlations of both PSM and WLH with both u and HLS suggests that both u and HLS data are similarly affected. The plot indicates that the data meet modern standards in terms of their coherence after about 1886, but there is a detectable decline as one goes back in time before then. If the plot is taken at face value it implies that the magnetometry techniques improved rather considerably over a rather short interval (about 7 yr between 1887 and 1894). Note the need to use annual correction factors on the Greenwich data mean that we cannot apply the same tests to monthly data.

Also shown is the correlation between u and IDV(1d)$_{HLS}$ (black/green line). The decay in quality of both u and IDV(1d)$_{HLS}$ around 1883, as inferred by comparison with the WLH and PSM data, is seen as a deeper minimum in the variation of this correlation. Earlier still, this correlation shows considerable variability, reaching almost the modern levels around 1880 but with another deep minimum around 1877. There is no categorical way of knowing if this difference arises from u or the Helsinki data or both.

8 Discussion and conclusions

We have presented a new composite of geomagnetic activity based on interdiurnal variability in the observed horizontal component of the geomagnetic field. The aim is that the composite is as close to homogeneous in its construction as it possibly can be: it uses data from Helsinki for 1846–1890 (inclusive) and 1893–1897 and from Eskdalemuir from 1911 to the present day. The gaps are filled using data from the Potsdam (1891–1892 and 1898–1907) and the nearby Seddin observatories (1908–1910) and intercalibration achieved using the Potsdam–Seddin sequence (1890–1931). We revert to using the interdiurnal variation between daily means (as employed by Bartels, 1932), rather than just the midnight value used in IDV, and we name the index derived as IDV(1d) to avoid potential confusion. Allowance has been made for the effects of secular changes in the geomagnetic field on the geomagnetic latitude of the stations used. The uncertainties in the composite due to the necessary intercalibrations of the stations have been computed. In all cases, we have ensured that regression fits used are homoskedastic and unbiased and that the fit residuals follow a normal distribution, as required for least-squares fitting.

The composite has been tested against independent early data from Greenwich, St Petersburg, Parc St Maur, Ekaterinburg and the composite u index, compiled from 1–6 stations by Bartels (1932). For the 20th century it is tested against the IDV index of SC10. In order to do this we have digitised the data from the Greenwich yearbooks and applied the temperature correction to annual values, rather than to each hourly mean. Agreement between these other data and the IDV(1d) composite was found to be extremely good in all cases, with two exceptions.

Firstly, the Greenwich data are shown to have degraded in quality, even in annual means, after about 1890 until new instrumentation was installed in 1915. We note that Bartels (1932) had similar misgivings about the Greenwich data. Secondly, we find that the Bartels u index does not agree at all well with the Helsinki data before about 1880, with the solar cycle amplitudes and the average level geomagnetic activity before then considerably greater in u. Before 1872, u is based on proxy data rather than interdiurnal variability and, as previously discussed, Bartels himself did not regard these data as satisfactory. After 1886, u agrees very well the Helsinki data (until the noise problem at the Helsinki site degrades the quality of the data after 1896). We here find the u data between 1872 and 1886 also shows solar cycles greater in amplitude than is seen in the Helsinki data (see the lower panel in Fig. 13). This would also explain the larger cycles in u before 1872 because the s and E proxies used before 1872 have been fitted to solar cycles in u that are too large in amplitude.

The one firm conclusion we can make is that the u index (and hence IDV) and the Helsinki data are not in such good agreement before 1886. There is no definitive test that allows us to state, with total certainty, the relative contributions that their respective errors make to the discrepancy. However there are a number of reasons to place much greater faith in the Helsinki data. The Helsinki data are a homogeneous set of continuous measurements made for 70 yr from the same site with the same equipment and using the same procedures (Nevanlinna, 2004; Nevanlinna and Häkkinen, 2010). On the other hand, u is compiled from a mixture of sources and relies on proxies for the interdiurnal variation before 1872. Before the start of the Batavia data in 1884, the actual interdiurnal variation data between 1872 and 1884 is taken from Greenwich and Bombay. We here find the stability of the Greenwich data to be poor and variable, as did Bartels and he ascribed Greenwich lower weighting in u as a result. We also note Bartels expressed concerns about the effects of many data gaps on the monthly means of some of the early Bombay data and ascribes that station half weighting also at such times. Thus for much of the early interval, u is based on Bombay and Greenwich data with weightings of 1 and 0.5, respectively. A point to note is that u uses whole-day means (as does IDV(1d) but unlike IDV) and the analysis for low-latitude modern data shown in Fig. 3 reveals that the Bombay u data will have had a peak response of about $BV^{-0.4}$

whereas the Greenwich data will have had a peak response close to $BV^{-0.2}$. This means that fast speed flow streams which raise annual means of V will cause u to be lower than an index with a peak response of B. This fits with the differences between u (and hence IDV) and IDV(1d) (and the Russian stations) in the declining phases of the solar cycles. The u index also mixes midlatitude and equatorial stations and so the range of latitude correction factors is large. Using the Λ values from geomagnetic field models for the stations and the empirical dependence of station responses in modern times we make allowance for the secular drift in the station locations. The one direct test that we have been able to make is that the earliest Helsinki data agree very well with interdiurnal variation data from the Russian observatories, St Petersburg, Nertchinsk and Barnaul (Nevanlinna and Häkkinen, 2010), whereas the u index data (at this time based on the proxies) do not. Hence we think that Bartels' warnings that the pre-1872 data should be regarded as unsatisfactory and illustrative are both well-founded and wise.

This paper is the first of a series of three. In Part 2 (Lockwood et al., 2013a) we employ the composite described here to reconstruct the interplanetary magnetic field (IMF) from 1845 to the present day. In Part 3 (Lockwood et al., 2013b), we construct a range index composite that is as homogeneous as it can be and apply the method of Lockwood et al. (1999) (as adapted by Lockwood and Owens (2011) to yield the near-Earth IMF rather than the open solar flux) and compare the results with those of Part 2.

References

Barraclough, D. R.: Spherical Harmonic Analyses of the Geomagnetic Field for Eight Epochs between 1600 and 1910, Geophysical J. of the R.A.S., 36, 497–513, doi:10.1111/j.1365-246X.1974.tb00611.x, 1974.

Barraclough, D. R.: Spherical harmonic models of the geomagnetic field, Inst. Geol. Sci., Geomagn. Bull., 8., Stationery Office Books (London), ISBN-10: 0118812696, ISBN-13: 9780118812696, 1978.

Bartels, J.: Terrestrial-magnetic activity and its relations to solar phenomena, Terr. Magn. Atmos. Electr., 37, 1–52, doi:10.1029/TE037i001p00001, 1932.

Bartels, J., Heck, N. H., and Johnston, H. F.: The three-hour-range index measuring geomagnetic activity, J. Geophys. Res., 44, 411–454, doi:10.1029/TE044i004p00411, 1939.

Brum, C. G. M., Tepley, C. A., Fentzke, J. T., Robles, E., dos Santos, P. T., and Gonzalez, S. A.: Long-term changes in the thermospheric neutral winds over Arecibo: Climatology based on over three decades of Fabry-Perot observations , J. Geophys. Res., 117, A00H14, doi:10.1029/2011JA016458, 2012.

Clilverd, M. A., Clark, T. D. G., Clarke, E., and Rishbeth, H.: Increased magnetic storm activity from 1868 to 1995, J. Atmos. Sol.-Terr. Phy., 60, 1047–1056, doi:10.1016/S1364-6826(98)00049-2, 1998.

Clilverd, M. A., Clarke, E., Ulich, T., Linthe, J.-H., and Rishbeth, H.: Reconstructing the long-term aa index, J. Geophys. Res., 110, A07205, doi:10.1029/2004JA010762, 2005.

Cnossen, I. and Richmond, A. D.: Changes in the Earth's magnetic field over the past century: Effects on the ionosphere-thermosphere system and solar quiet (Sq) magnetic variation, J. Geophys. Res., 118, 849–858, doi:10.1029/2012JA018447, 2013.

Feynman, J. and Crooker, N. U.: The solar wind at the turn of the century, Nature, 275, 626–627, doi:10.1038/275626a0, 1978.

Finch, I. and Lockwood, M.: Solar wind-magnetosphere coupling functions on timescales of 1 day to 1 year, Ann. Geophys., 25, 495–506, doi:10.5194/angeo-25-495-2007, 2007.

Finch, I. D., Lockwood, M., and Rouillard, A. P.: Effects of solar wind magnetosphere coupling recorded at different geomagnetic latitudes: Separation of directly-driven and storage/release systems, Geophys. Res. Lett., 35, L21105, doi:10.1029/2008GL035399, 2008.

Finlay, C. C., Maus, S., Beggan, C. D., Bondar, T. N., Chambodut, A., Chernova, T. A., Chulliat, A., Golovkov, V. P., Hamilton, B., Hamoudi, M., Holme, R., Hulot, G., Kuang, W., Langlais, B., Lesur, V., Lowes, F. J., Lühr, H., Macmillan, S., Mandea, M., McLean, S., Manoj, C., Menvielle, M., Michaelis, I., Olsen, N., Rauberg, J., Rother, M., Sabaka, T. J., Tangborn, A., Tøffner-Clausen, L., Thébault, E., Thomson, A. W. P., Wardinski, I., Wei, Z., and Zvereva, T. I.: International Geomagnetic Reference Field: the eleventh generation, Geophys. J. Int., 183, 1216–1230, doi:10.1111/j.1365-246X.2010.04804.x, 2010.

Gustafsson, G., Papitashvili, N. E., and Papitashvili, V. O.: A Revised Corrected Geomagnetic Coordinate System for Epochs 1985 and 1990, J. Atmos. Terr. Phys., 54, 1609–1631, 1992.

Harrison, R. G.: Long term measurements of the global atmospheric electric circuit at Eskdalemuir, Scotland, 1911–1981, Atmos. Res., 70, 1–19, doi:10.1016/j.atmosres.2003.09.007, 2004.

Jackson, A., Jonkers, A. R., and Walker, M. R.: Four centuries of geomagnetic secular variation from historical records, Philos. T. Roy. Soc. A, 358, 957–990, doi:10.1098/rsta.2000.0569, 2000.

Kivelson, M. G. and Hughes, W. J.: On the threshold for triggering substorms, Planet. Space Sci., 38, 211–220, doi:10.1016/0032-0633(90)90085-5, 1990.

Lockwood, M.: Twenty-three cycles of changing open solar magnetic flux, J. Geophys. Res., 108, 1128, doi:10.1029/2002JA009431, 2003.

Lockwood, M.: Solar change and climate: an update in the light of the current exceptional solar minimum, Proc. R. Soc. A, 466, 303–329, doi:10.1098/rspa.2009.0519, 2010.

Lockwood, M.: Reconstruction and Prediction of Variations in the Open Solar Magnetic Flux and Interplanetary Conditions, Living Reviews in Solar Physics, 10, 4, doi:10.12942/lrsp-2013-4, 2013.

Lockwood, M. and Owens, M. J.: Centennial changes in the heliospheric magnetic field and open solar flux: the consensus view from geomagnetic data and cosmogenic isotopes and its implications, J. Geophys. Res., 116, A04109, doi:10.1029/2010JA016220, 2011.

Lockwood, M., Stamper, R., and Wild, M. N.: A doubling of the sun's coronal magnetic field during the last 100 years, Nature, 399, 437–439, doi:10.1038/20867, 1999.

Lockwood, M., Rouillard, A. P., Finch, I. D., and Stamper, R.: Comment on The IDV index: its derivation and use in inferring long-term variations of the interplanetary magnetic field strength by Svalgaard and Cliver, J. Geophys. Res., 111, A09109, doi:10.1029/2006JA011640, 2006a.

Lockwood, M., Whiter, D., Hancock, B., Henwood, R., Ulich, T., Linthe, H. J., Clarke, E., and Clilverd, M.: The long-term drift in geomagnetic activity: calibration of the aa index using data from a variety of magnetometer stations, Rutherford Appleton Laboratory (RAL), Harwell Oxford, UK, http://www.eiscat.rl.ac.uk/Members/mike/publications/pdfs/sub/241_Lockwood_aa_correct_S1a.pdf, 2006b.

Lockwood, M., Rouillard, A. P., and Finch, I. D.: The rise and fall of open solar flux during the current grand solar maximum, Astrophys. J., 700, 937–944, doi:10.1088/0004-637X/700/2/937, 2009.

Lockwood, M., Owens, M. J., Barnard, L., Davis, C. J., and Thomas, S.: Solar cycle 24: What is the Sun up to?, Astron. Geophys., 53, 3.09–3.15, doi:10.1111/j.1468-4004.2012.53309.x, 2012.

Lockwood, M., Barnard, L., Nevanlinna, H., Owens, M. J., Harrison, R. G., Rouillard, A. P., and Davis, C. J.: Reconstruction of geomagnetic activity and near-Earth interplanetary conditions over the past 167 yr – Part 2: A new reconstruction of the interplanetary magnetic field, Ann. Geophys., 31, 1979–1992, doi:10.5194/angeo-31-1979-2013, 2013a.

Lockwood, M., Barnard, L., Nevanlinna, H., Owens, M. J., Harrison, R. G., Rouillard, A. P., and Davis, C. J.: Reconstruction of geomagnetic activity and near-Earth interplanetary conditions over the past 167 years: 3. A new range index composite and reconstruction of solar wind speed, in preparation, 2013b.

Love, J. J.: Long-term biases in geomagnetic K and aa indices, Ann. Geophys., 29, 1365–1375, doi:10.5194/angeo-29-1365-2011, 2011.

Malin, S. R. C.: Geomagnetism at the Royal Observatory, Greenwich, Q. J. Roy. Astron. Soc. London, 37, 65–74, 1996.

Martini, D. and Mursula, K.: Correcting the geomagnetic IHV index of the Eskdalemuir observatory, Ann. Geophys., 24, 3411–3419, doi:10.5194/angeo-24-3411-2006, 2006.

Mayaud, P.-N.: Une mesure planétaire d'activité magnétique, basée sur deux observatoires antipodaux, Ann. Geophys., 27, 67–70, 1971.

Mayaud, P.-N.: The *aa* indices: A 100-year series characterizing the magnetic activity, J. Geophys. Res., 77, 6870–6874, doi:10.1029/JA077i034p06870, 1972.

Mayaud, P.-N.: Derivation, Meaning and Use of Geomagnetic Indices, Geophysical Monograph, 22, American Geophysical Union, Washington, DC, doi:10.1029/GM022, 1980.

Macmillan, S. and Clarke, E.: Resolving issues concerning Eskdalemuir geomagnetic hourly values, Ann. Geophys., 29, 283–288, doi:10.5194/angeo-29-283-2011, 2011.

Moen, J. and Brekke, A.: The solar flux influence on quiet time conductivities in the auroral ionosphere, Geophys, Res. Lett., 20, 971–974, 1993.

Mursula, K. and Martini, D.: Centennial increase in geomagnetic activity: Latitudinal differences and global estimates, J. Geophys. Res., 111, A08209, doi:10.1029/2005JA011549, 2006.

Mursula, K., Martini, D., and Karinen, A.: Did Open Solar Magnetic Field Increase During The Last 100 Years? A Reanalysis of Geomagnetic Activity, Solar Phys., 224, 85–94, doi:10.1007/s11207-005-4981-y, 2004.

Nevanlinna, H.: Results of the Helsinki magnetic observatory 1844–1912, Ann. Geophys., 22, 1691–1704, doi:10.5194/angeo-22-1691-2004, 2004.

Nevanlinna, H.: A study on the great geomagnetic storm of 1859: Comparisons with other storms in the 19th century, Adv. Space Res., 38, 180–187, doi:10.1016/j.asr.2005.02.102, 2006.

Nevanlinna, H. and Häkkinen, L.: Results of Russian geomagnetic observatories in the 19th century: magnetic activity, 1841–1862, Ann. Geophys., 28, 917–926, doi:10.5194/angeo-28-917-2010, 2010.

Nevanlinna, H. and Kataja, E.: An extension of the geomagnetic activity index series *aa* for two solar cycles (1844–1868), Geophys. Res. Lett., 20, 2703–2706, doi:10.1029/93GL03001, 1993.

Nowada, M., Shue, J.-H., and Russell, C. T.: Effects of dipole tilt angle on geomagnetic activity, Planet. Space Sci., 57, 1254–1259, doi:10.1016/j.pss.2009.04.007, 2009.

Richter, P. H.: Estimating Errors in Least-Squares Fitting, in: The Telecommunications and Data Acquisition Progress Report 42-122, edited by: Yuen, J. H., NASA Code 314-30-42-01-14, http://tmo.jpl.nasa.gov/progress_report/42-122/122E.pdf, 1995.

Rouillard, A. P., Lockwood, M., and Finch, I. D.: Centennial changes in the solar wind speed and in the open solar flux, J. Geophys. Res., 112, A05103, doi:10.1029/2006JA012130, 2007.

Russell, C. T.: The universal time variation of geomagnetic activity, Geophys. Res. Lett., 16, 555–558, doi:10.1029/GL016i006p00555, 1989.

Russell, C. T. and McPherron, R. L.: Semiannual variation of geomagnetic activity, J. Geophys. Res., 78, 92–108, doi:10.1029/JA078i001p00092, 1973.

Stamper, R., Lockwood, M., Wild, M., and Clark, T.: Solar Causes of the Long Term Increase in Geomagnetic Activity, J. Geophys. Res., 104, 28325–28342, doi:10.1029/1999JA900311, 1999.

Svalgaard, L. and Cliver, E. W.: The IDV index: Its derivation and use in inferring long-term variations of the interplanetary magnetic field strength, J. Geophys. Res., 110, A12103, doi:10.1029/2005JA011203, 2005.

Svalgaard, L. and Cliver, E. W.: Interhourly variability index of geomagnetic activity and its use in deriving the long-term variation of solar wind speed, J. Geophys. Res., 112, A10111, doi:10.1029/2007JA012437, 2007.

Svalgaard, L. and Cliver, E. W.: Heliospheric magnetic field 1835–2009, J. Geophys. Res., 115, A09111, doi:10.1029/2009JA015069, 2010.

Svalgaard, L., Cliver, E. W., and Le Sager, P.: Determination of interplanetary magnetic field strength, solar wind speed and EUV irradiance, 1890–2003, in: Solar Variability as an Input to the Earth's Environment, edited by: Wilson, A., ESA Special Publication, 535, 15–23, European Space Agency, Nordwijk, 2003.

Svalgaard, L., Cliver, E. W., and Le Sager, P.: IHV: a new long-term geomagnetic index, Adv. Space Res., 34, 436–439, doi:10.1016/j.asr.2003.01.029, 2004.

van Storch, H. and Zwiers, F. W.: Statistical Analysis in Climate Research, Chapter 8, Cambridge Univ. Press, New York, 1999.

Wallis, D. D. and Budzinski, E. E.: Empirical models of height integrated conductivities, J. Geophys. Res., 86, 2156–2202, doi:10.1029/JA086iA01p00125, 1981.

Wilks, D. S.: Statistical Methods in the Atmospheric Sciences, Chapter 6, Elsevier, New York, 1995.

Yamazaki, Y., Yumoto, K., Cardinal, M. G., Fraser, B. J., Hattori, P., Kakinami, Y., Liu, J. Y., Lynn, K. J. W., Marshall, R., McNamara, D., Nagatsuma, T., Nikiforov, V. M., Otadoy, R. E., Ruhimat, M., Shevtsov, B. M., Shiokawa, K., Abe, S., Uozumi, T., and Yoshikawa, A.: An empirical model of the quiet daily geomagnetic field variation, J. Geophys. Res., 116, A10312, doi:10.1029/2011JA016487, 2011.